CHAPTER II

INSTRUMENTS, MATERIALS, AND METHODS

II.1 Instruments

Mettler FP5: Control Unit

Mettler FP52: Hot stage for microthermal investigations with a hand control panel

Olympus trinocular microscope, with two 10x oculars and x4, x10, x20 objectives, including a polarizer

Olympus micrographic camera, model PM6, with a x10 planar eyepiece

Olympus photomicrographic exposure meter, model EMM-V

Nikon trinocular microscope model L-Ke with two 10x oculars and a x10 objective including a polarizer, an analyzer and a blue filter

II.2 Materials

Liquid Crystals (The abbreviated name and catalogue number are in parentheses):

p-Azoxyanisole (PAA), from Aldrich Chemical Co., Inc.(9700)

p,p'-di-Hexyloxyazoxybenzene (PHAB), from Frinton Laboratories (648)

p-((p-Methoxybenzylidine) amino) phenyl acetate (MBAPA), from Frinton Laboratories (761)

p-Azoxyphenetole (PAP), from Riedel Co. (9781)

The following chemicals were purchased from Eastman Kodak Co.

n-Butyl p-(p-Ethoxyphenoxycarbonyl) phenyl carbonate (BEPCPC) (10482)

p-(p-Ethoxyphenylazo) phenyl n-hexanoate (EPP-Hex)(10537)

p-(p-Ethoxyphenylazo) phenyl n-heptanoate(EPP-Hep)(10573)

p-(p-Ethoxyphenylazo) phenyl n-undecylenate (EPPU)(10541)

p-(p-Ethoxyphenylazo) phenyl valerate (EPPV) (10901)

p-(p-Ethoxyphenylazo) phenyl crotonoate (EPPC) (10836)

p,p'-Bis(heptyloxy) azoxybenzene (PBHAB) (10122)

p,p'-Bis(pentyloxy) azoxybenzene (PBPAB) (10715)

p,p'-Dipropoxyazoxybenzene (PDPAB) (10714)

p,p'-Dibutoxyazoxybenzene (PDBAB) (10717)

p,p'-Azodiphenetole (PAD) (9857)

p-((p-Methoxybenzylidine) amino) benzonitrile (MBAB) (10880)

N-(p-Methoxybenzylidine)-p-phenylazoaniline (MBPPA) (8545)

p-Anisaldazine (PASA) (8546)

All of these compounds were used as obtained without further purification. Only EPP-Hep and EPP-Hex, which had wide ranges of melting point, were recrystallized before using.

Films

Agfa Super Pan ASA 200, 35 mm.

Kodak Tri-X-Pan ASA 400, 35 mm.

Table 1 Names, formulae, abbreviations and the nematic temperature ranges of the liquid crystals used.

Name and Formula	Abbreviation	Nematic-range(°C)
p,p'-Bis(pentyloxy) azoxybenzene 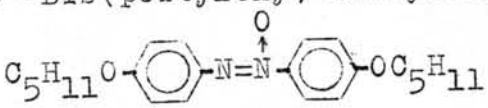	PBPAB	77.1-119.9
p,p'-Dipropoxyazoxybenzene 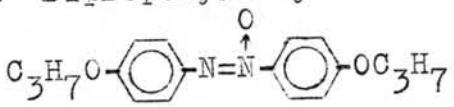	PDPAB	118.1-122.4
p,p'-Dibutoxyazoxybenzene 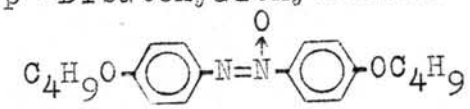	PDBAB	104.1-135.9
p,p'-Azoxydiphenetole 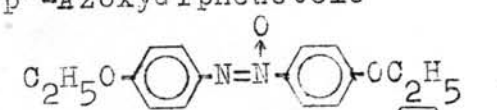	PAP	137.9-166.7
p-Azoxyanisole 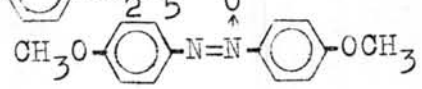	PAA	117.9-135.3
p,p'-Azodiphenetole 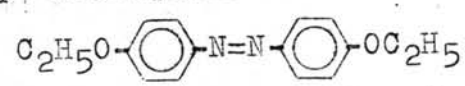	PAD	137.9-162.5
p-((p-Methoxybenzylidine) amino) benzonitrile 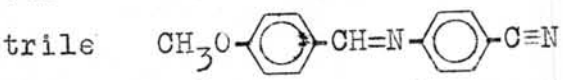	MBAB	106.4-118.4
p-((p-Ethoxybenzylidine) amino) benzonitrile 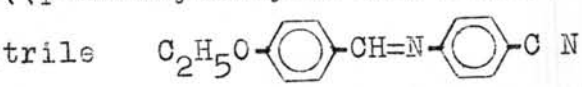	EBAB	105.6-127.9
N-(p-Methoxybenzylidine)-p-phenylazoaniline 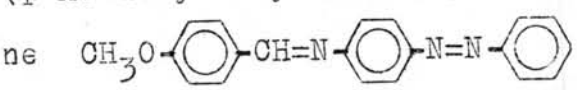	MBPPA	148.0-186.7
N-(p-Pentylcarbonyloxy benzylidine-p-anisidine 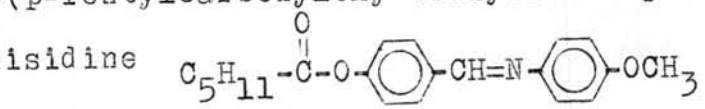	PCBPA	61.2-85.2

Name and Formula	Abbreviation	Nematic range (°C)
p-(p-Ethoxyphenylazo) phenyl valerate 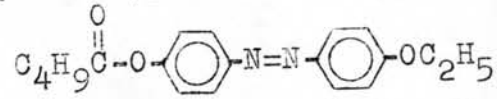	EPPV	78.1-127.3
p-(p-Ethoxyphenylazo) phenyl-n-heptanoate 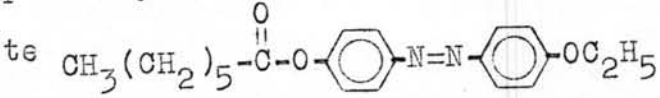	EPP-Hep	65.6-115.6
p-(p-Ethoxyphenylazo) phenyl-n-hexanoate 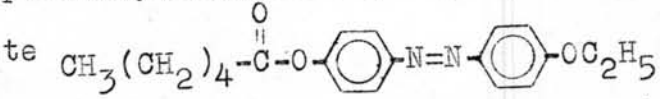	EPP-Hex	65.7-128.6
p-(p-Ethoxyphenylazo) phenylcrotonoate 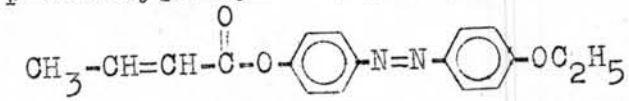	EPPC	110.5-193.9
p-(p-Ethoxyphenylazo) phenyl-n-undecylenate 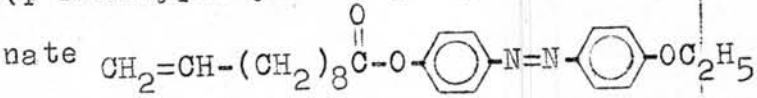	EPPU	65.5-107.9

II.3 Preparation of Samples

II.3.1 Preparation of mixtures.

All the mixtures to be investigated, i.e., the systems EPP-Hep/EPP-Hex, EPP-Hep/PAA, were prepared in the required mole percent compositions as follows. The two weighed components were mixed in a test tube and heated in a paraffin bath until the mixture became isotropic. It was cooled suddenly in an ice-water bath, the mixture being stirred vigorously until the mixture was frozen. Then the mixture was ready for the experiment.

II.3.2 Preparation of slides.

The microscope slides and cover slips were cleaned with acetone. A few pellicles of the liquid crystal to be investigated were put on the clean slide and melted on the heating stage before covering it with a cover slip. In this way, air bubbles could be removed from the specimen.

II.4 Experimental Methods

II.4.1 Determination of transition temperatures.

The prepared specimen was placed on the electronically controlled heating stage for microthermal investigations, mounted on the polarizing microscope. The illuminating beam of light was transmitted through the specimen to the objective. At high intensity of illumination, it was found that the light could raise the temperature of the specimen by as much as $0.1^{\circ}C$; thus the observation of the texture was sometimes interfered, especially in the vicinity of the transition temperature. This effect should be accounted for as a correction to the observed transition temperature. To minimize the nonuniform effects of light, the illuminating light was turned on for some time before the investigation. The temperature of the heating stage was read on the controller unit, which gave an accuracy of $0.1^{\circ}C$ and the heating rate as well as the cooling rate could be accurately controlled at any of the following rates: 10, 3, 2, 1 and $0.2^{\circ}C$/min.

It was found convenient to determine the transition temperature roughly first at a high heating rate, and then

to make the accurate determination. The temperature was increased at a moderate rate, 3-10°C/min, until the melting point was approached; then the rate was slowed down to 0.2°C/min. The temperature was held constant as soon as any physical change in the specimen could be observed, to make sure that there was no sharp change of the texture escaping notice. Usually, the transition point had a wide range, depending on the nature and range of pre-transition as well as on the purity of the sample. The melting temperature was recorded as soon as the last crystal was melted. Other transition temperatures were recorded as soon as a complete change of texture occurred. Since supercooling always occurred, heating and cooling gave different reverse sequences of textures.

In nematic liquid crystals, the marbled texture was observed over a very long range of temperature. In contrast, the range of observing the schlieren texture was usually narrow, and the reproducibility of the texture was found to be very sensitive to the intensity of the illuminating light. Its temperature range could not therefore be determined very accurately. Frequently, the marbled and the schlieren textures would coexist in the specimen at a particular temperature, indicating the slight inhomogenity of physical conditions and impurities in different parts of the specimen. Thus the transition temperature from the marbled to schlieren texture was recorded as soon as the first noticeable change of texture could be observed.

II.4.2 Observation of mesomorphic textures.

The textures of the mesomorphic phases were observed and photographed under crossed linear polarizations. The photographs were taken with the Olympus microscope camera mounted on the Nikon trinocular microscope model L-Ke with the magnification X100. To obtain sharp pictures, the blue filter normally inserted for visual observations was removed and a small aperture was chosen for the beam of transmitted light. High-sensitivity films were used for moving pictures.

The textures near the isotropic-nematic transition of mixtures and single nematic compounds have been compared.

II.4.3 Observation of schlieren texture.

The samples were carefully prepared for this purpose. The slides were cleaned in the cleaning solution (conc. H_2SO_4 and $K_2Cr_2O_7$) and washed with distilled water and then acetone. The slides were left to dry without any touch to avoid making scratches on the smooth surface that would induce a formation of the inversion walls. In non-recrystallized substances, the schlieren texture was usually observed even on a very clean slide. For recrystallized compounds, on the other hand, it was found sometimes necessary to prepare the sample on a dirty slide in order to obtain the schlieren texture.

To construct the inversion walls.

Two simple techniques were found to be effective in inducing a formation of the inversion walls.

i) The slide was rubbed several times along the long axis on a sheet of clean paper in one direction. The inversion walls were then formed parallel to the direction of rubbing.

ii) The substance was first melted between the slide and cover slip. The cover slip was then displaced slightly in the direction parallel to the long axis of the slide. By this method, the inversion walls were formed along the direction of displacement.

II.4.4 Investigation of the growth rate of nematic droplets.

On heating the sample up to the isotropic phase, the temperature was decreased slowly at the rate of $0.2^{\circ}C$/min. At sufficiently near the isotropic-nematic transition temperature, the temperature was kept constant. It was then waited until the droplets appeared. The diameter of a droplet was read from the micro-vernier eyepiece of the microscope with the magnification x60 at every ten seconds. Since the growth was very fast at the beginning, it was rather difficult to determine the initial diameter of the droplet. Usually, the starting time (t=0) always corresponded to some finite size of droplets. It was usually not possible to determine the growth rate of the same droplets that had previously been studied, because supercooling and hysteresis always took place. Moreover, the isotropic-nematic transition temperature became lower and lower with the repeated heating and cooling. Thus,

the growth rates of different droplets were determined at different times.

II.5 Experimental Results

II.5.1 Transition temperatures

a) The transition temperatures of various phases and modifications of the nematic liquid crystals that readily exhibited the schlieren texture are shown in the following tables:

Table 2 The transition temperatures of the nematic liquid crystals that readily exhibited the schlieren texture.

Liquid Crystals	melting pt. (°C)	marbled range (°C)	schlieren range(°C)	isotropic(°C)
PBPAB	76.3-77.1	77.1-119.6	119.6-119.9	119.9
PDPAB	115.1-118.1	118.1-120.1	120.1-122.4	122.4
PDBAB	99.8-104.1	104.1-135.8	135.8-135.9	135.9
PAD	130.9-137.9	137.9-155.3	155.3-162.5	162.5
MBAB	102.9-106.4	106.4-118.1	118.1-118.4	118.4
EBAB	104.9-105.6	105.6-126.6	126.6-127.9	127.9
MBPPA	140.7-148.0	148.0-186.2	186.2-186.7	186.7
PAA	117.4-117.9	117.9-135.2	135.2-135.3	135.3
PCBPA	60.1-61.2	61.2-84.8	84.8-85.2	85.2
PASA	151.4-169.8	169.8-181.9	181.9-182.5	182.5

b) The transition temperatures of nematic liquid crystals that did not exhibit the schlieren texture in the pure state, are given in the following table:

Table 3 The transition temperatures of nematic liquid crystals that did not exhibit the schlieren texture in the pure state.

Liquid Crystals	melting pt.(°C)	marbled range(°C)	isotropic(°C)
EPPV	76.3-78.1	78.1-127.3	127.3
EPP-Hex	64.7-65.7	65.7-128.6	128.6
EPP-Hep	65.0-65.6	65.6-115.6	115.6
EPPC	103.6-110.5	110.5-193.9	193.9
EPPU	63.0-65.5	65.5-107.9	107.9
PAP	137.0-137.9	137.0-166.7	166.7

The temperature range of the melting point was determined by the nature of pre-transition and the presence of impurities.

II.5.2 Observation of the mesomorphic textures

i. Observation of nematic textures.

Nematic liquid crystals in the state of thin layers can exhibit three distinct nematic modifications cr textures, viz., the marbled texture, the schlieren texture, and the pseudo-isotropic state. The pseudo-isotropic state is always observed near the mesomorphic-isotropic transition on a clean slide. It is evident that not all nematic liquid crystals in the very pure state exhibit the schlieren texture. From the present

investigation of some twenty nematogenic substances, six of them do not under normal conditions show the schlieren texture, independent of the rate of cooling or heating. However, every nematic compound shows the schlieren texture if the specimen is prepared on a dirty slide. For example, when EPP-Hex and EPP-Hep were recrystallized before using, no schlieren texture was observed except when the samples were put on dirty slides (see Figs.6b, c, d and 7c).

Pure nematic compounds exhibited the marbled texture with very few lines of discontinuity, where threads were hardly observed. The number of disclination lines increased with the increased amount of impurities. At higher temperatures bright loops of threads disappeared without any trace. In single-texture nematic compounds sufficiently near the nematic-isotropic transition temperature, droplets with coloured rings seemed to emerge from the nematic surface. Figs.6b and 7b show the examples of these rings. Sharp dark lines which did not rotate with respect to the polarizer were always observed. The number of the circles increased as the temperature. As the rings grew larger and larger, the spaces between the outer rings became smaller than those near the centre. At some critical sizes, they blew out; that is, they became isotropic. The process was repeated again and again until all the marbled regions became isotropic .

On cooling from the isotropic to the nematic phase, nematic droplets were formed. These droplets looked flat and

were not so round. The droplets did not move; it appeared that they were stuck on to the glass surface (Fig.6c). The droplets grew rapidly and the marbled texture would be formed as a whole in a very narrow temperature range. Lines of discontinuity sometimes appeared at the contact area, but they were usually diminished in a moment.

When EPP-Hex (recryst.) was prepared on a dirty slide, a large number of line discontinuities could be observed in the marbled texture (Fig.6d), accompanied by the schlieren

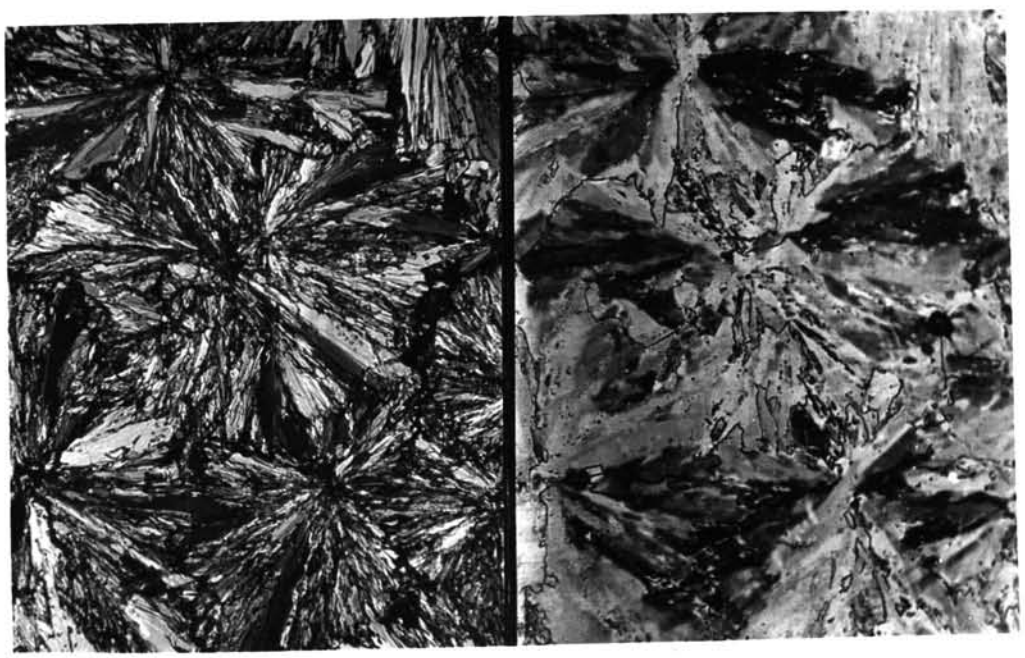

(i) (ii)

Fig.6a Texture of EPP-Hex (recryst.) in the solid phase (i) and the corresponding marbled texture at 65.8°C (ii).

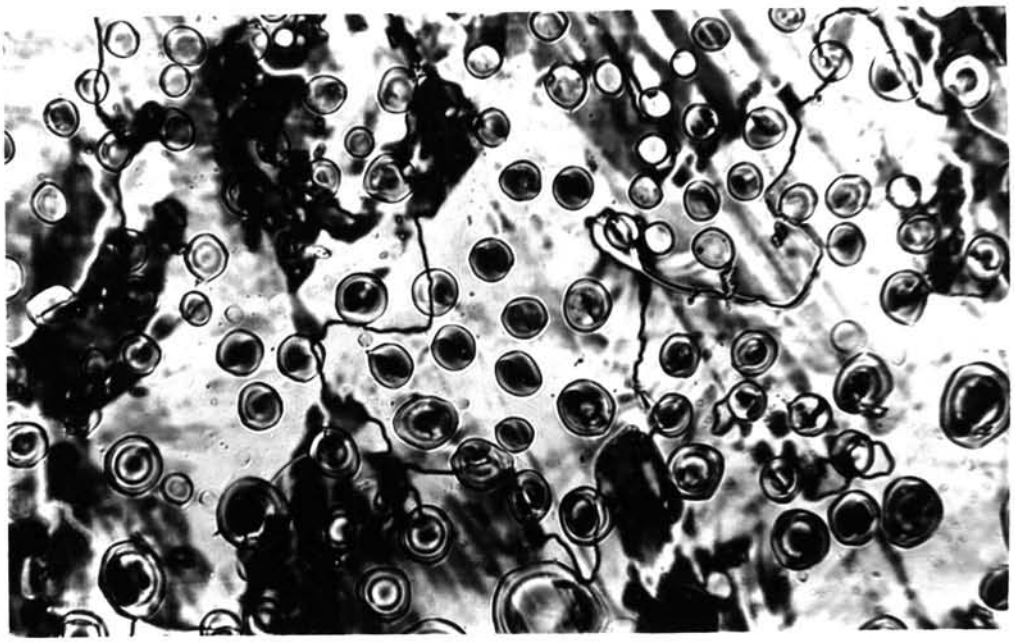

Fig.6b Texture of EPP-Hex (recryst.) at the nematic-isotropic transition at 128.4°C, under crossed polarizers.

texture in the immediate vicinity of the nematic-isotropic transition point (Figs.6d and 7c). Round nematic droplets were formed with point singularities inside them. It should be noted that in Fig.7c point singularities are formed at the impurities.

The transition temperatures of the pure samples and of the dirty samples were not very much different.

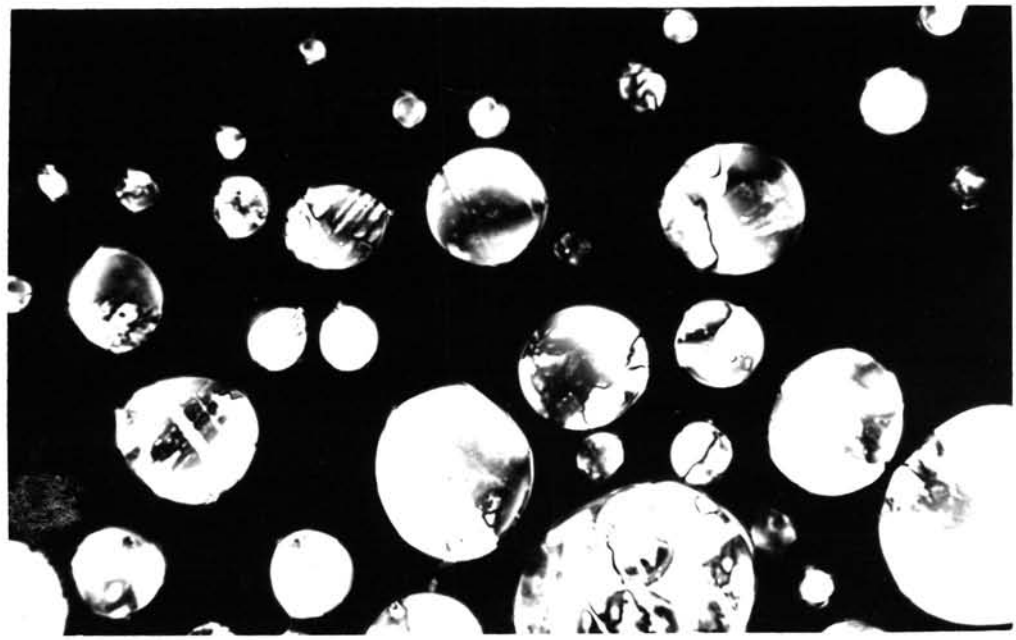

Fig.6c Isotropic-nematic transition of EPP-Hex (recryst.) at 128.5°C under crossed polarizers. These droplets show the marbled texture.

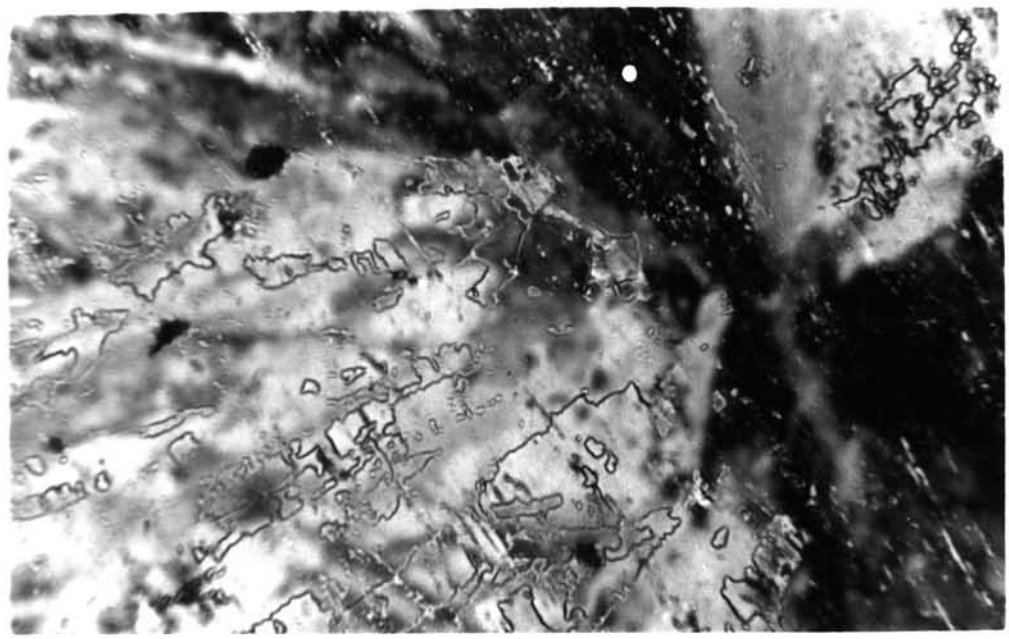

Fig.6d Marbled texture formed on dirty slide of EPP-Hex(recryst. Lines of discontinuity are observed.

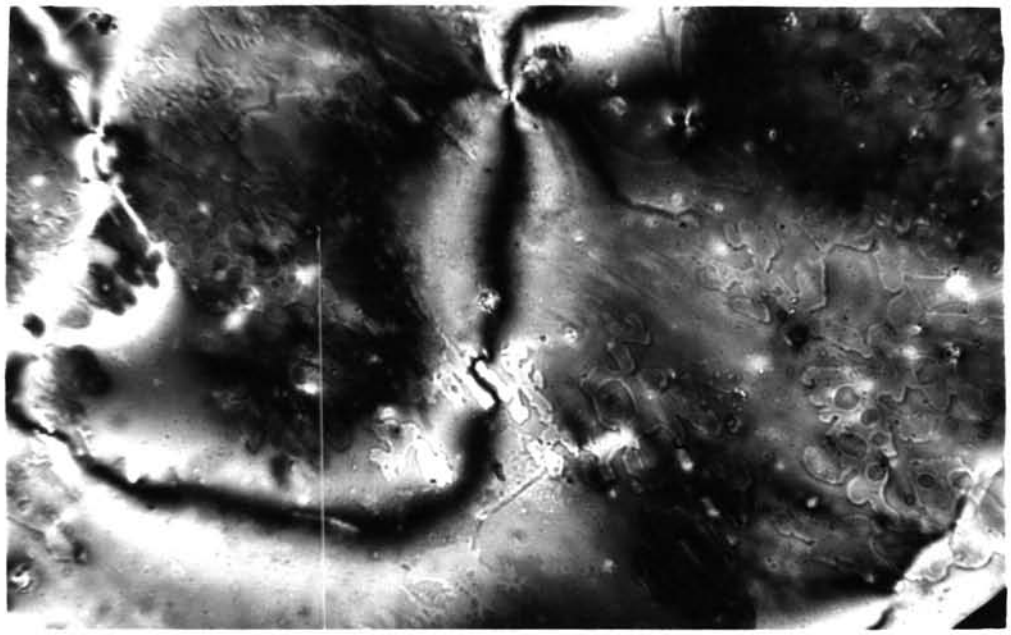

Fig.6e Schlieren texture formed on dirty slide by EPP-Hex (recryst.) at 128.5°C.

Fig.7a Marbled texture of EPPV at 122.6°C. Crossed polarizers.

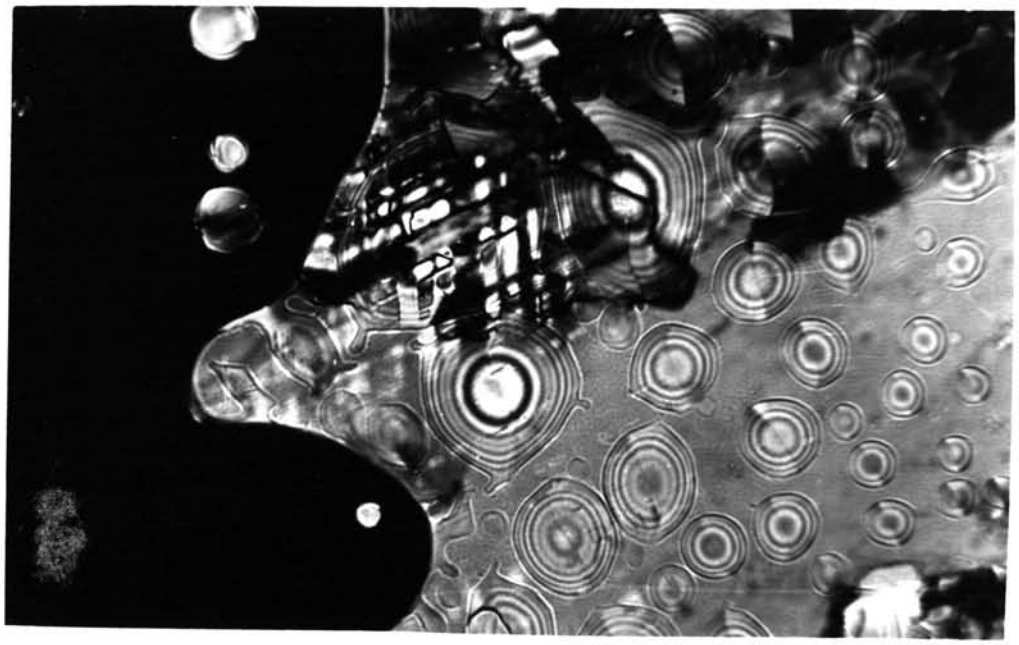

Fig.7b Nematic-isotropic transition of EPPV at 127.2°C. Concentric rings can be observed.

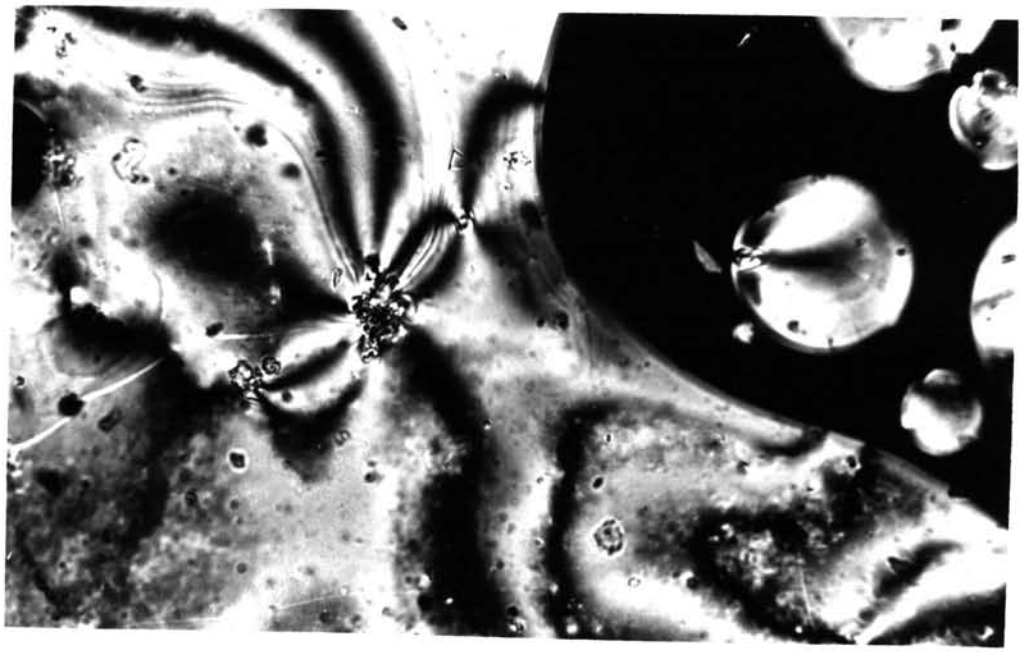

Fig.7c Isotropic-nematic transition of EPPV on dirty slide at 127.1°C. Point singularities are formed at the impurities.

ii Observation of schlieren texture

Annihilation and creation of point singularities were observed near the nematic-isotropic transition temperature. Brushes of the schlieren texture always corresponded to dark lines in the marbled texture. Figs.8a and 8b show the creation of singularities and brushes from the disclination lines in the marbled texture. These sharp lines did not rotate with respect to the polarizer. Near the marbled-schlieren transition the sharp lines were enlarged and began to rotate around the singular points. At higher temperatures rings could always be seen around these points. Sometimes sharp bright lines were also created almost parallel to the schlieren brushes. Their ends always disappeared at the point singularities while the other ends traversed to the surface. Sometimes they joined the two singularities and shrank in length at higher temperatures; as a result, the singularity pairs were annihilated. These bright lines did not rotate with respect to the polarizer and diminished at higher temperatures.

Figs.8c, d, e show the annihilation of a pair of +1 and -1 point singularities. A bright dot was left after the annihilation. The sharp bright loop around the dipoles was also diminished.

The number of brushes observed at each singularity was always two or four; a singularity with the number of brushes that differred from this was not stable. The excess brushes were always eliminated by splitting of the point singularities

or by diminishing of these brushes. Point singularities with only one brush were also observed at the isotropic-nematic interface; thus they were always observed in the nematic droplets. Such a point singularity changed its position along the nematic surface. Usually, all kinds of point singularities preferred to move towards the nematic surface.

The number of point singularities depended on the heating and cooling rate. The number was large at high cooling rate.

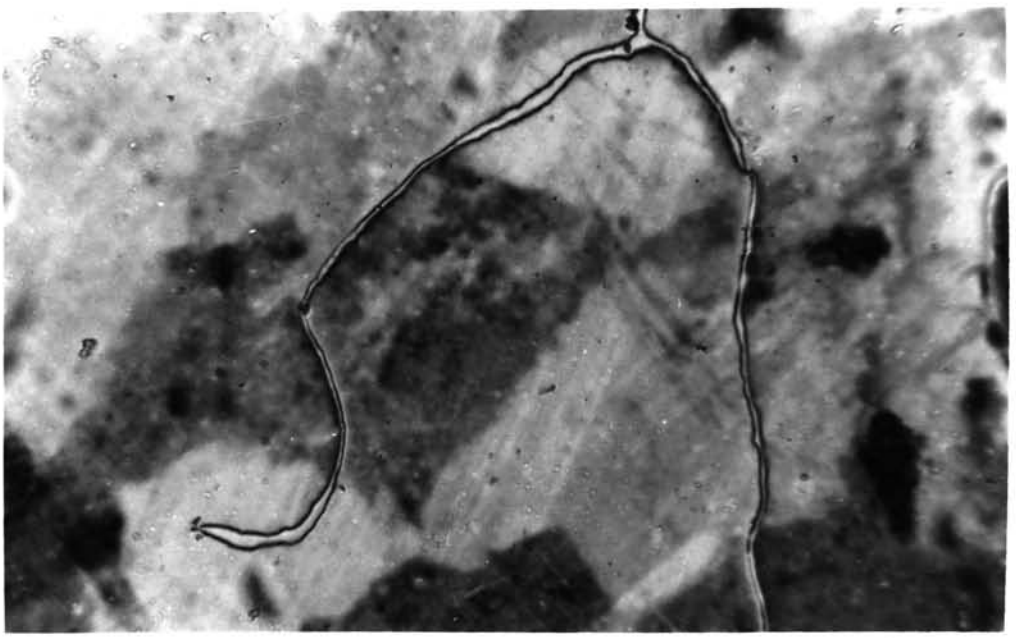

Fig.8a Marbled texture of PDBAB at 129.2°C. Sharp dark lines appear as a result of cooling from the isotropic to the nematic phase.

Fig.8b Schlieren texture of PDBAB at 135.6°C exhibited by the same sample as that shown in Fig.8a.

Fig.8c Schlieren texture in PDBAB at 135.8°C, with a pair of point singularities about to annihilate each other. Crossed polarizers.

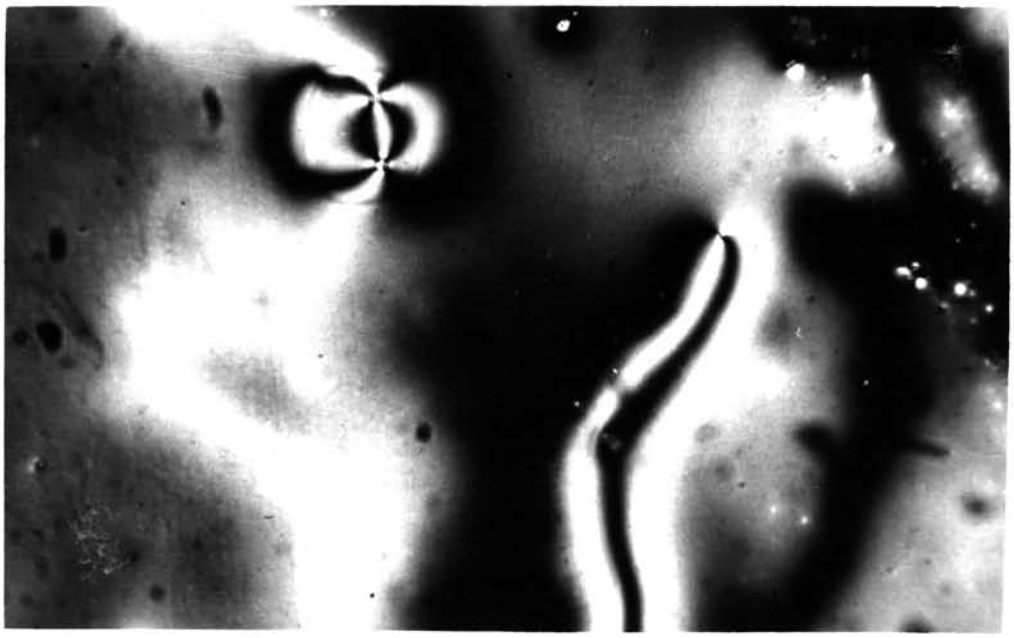

Fig.8d The same pair of point singularities as that shown in Fig.8c, just before the complete annihilation.

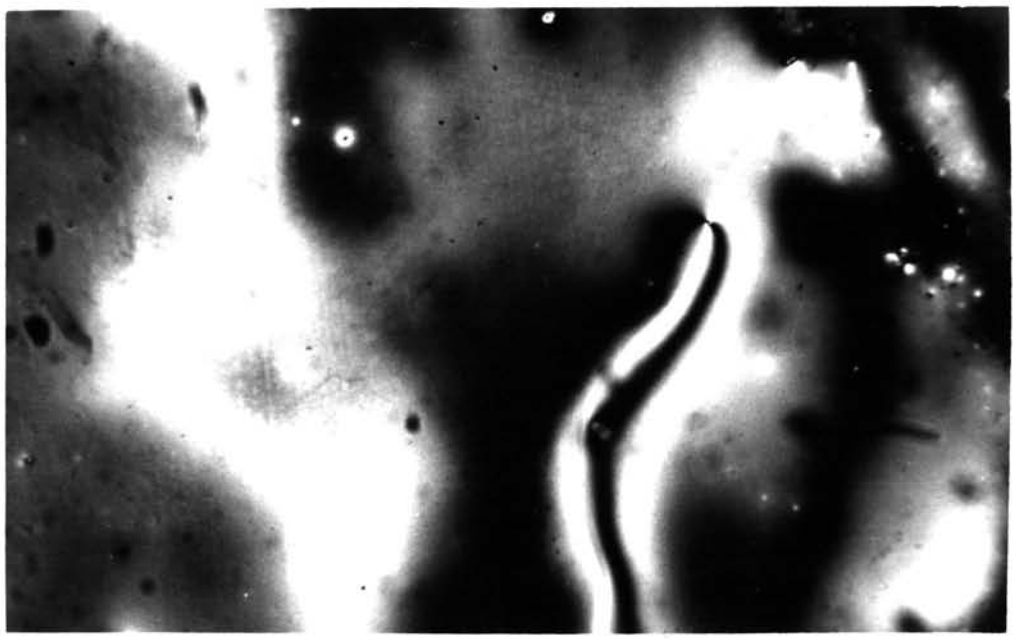

Fig.8e Complete annihilation of the pair of point singularities shown in Figs.8c and 8d. A bright dot is left after the annihilation.

Point singularities formed in the inversion walls were different from those formed elsewhere. Sharp dark lines joining between the singularities are seen in Figs.9a. Either side of the lines appears bright while the rest of the sample is dark. "The inversion wall of the first kind" could be observed as narrow parallel lines (see Fig.9a) ending at a $+\frac{1}{2}$ or $-\frac{1}{2}$ point singularity. Another kind, "the inversion wall of the second kind appeared as a sharp bright line joining the two point singularities, as shown in Fig.9b. As the temperature was increased, the lines shrank and two point singularities merged into one. Occasionally, these two kinds of inversion walls existed together in the same specimen.

The induced formation of the inversion walls obtained by rubbing the slides was sometimes found to be not as effective as that obtained by displacing the cover slip, especially when the slides were dirty. Fig.10 shows the schlieren texture of PDBAB on a dirty slide. The cover slip was displaced slightly and thousands of inversion lines were formed between the point singularities. When the temperature was raised, most of these singularities were annihilated and only a few were left. Black brushes could then be observed and these rotated around the singular points.

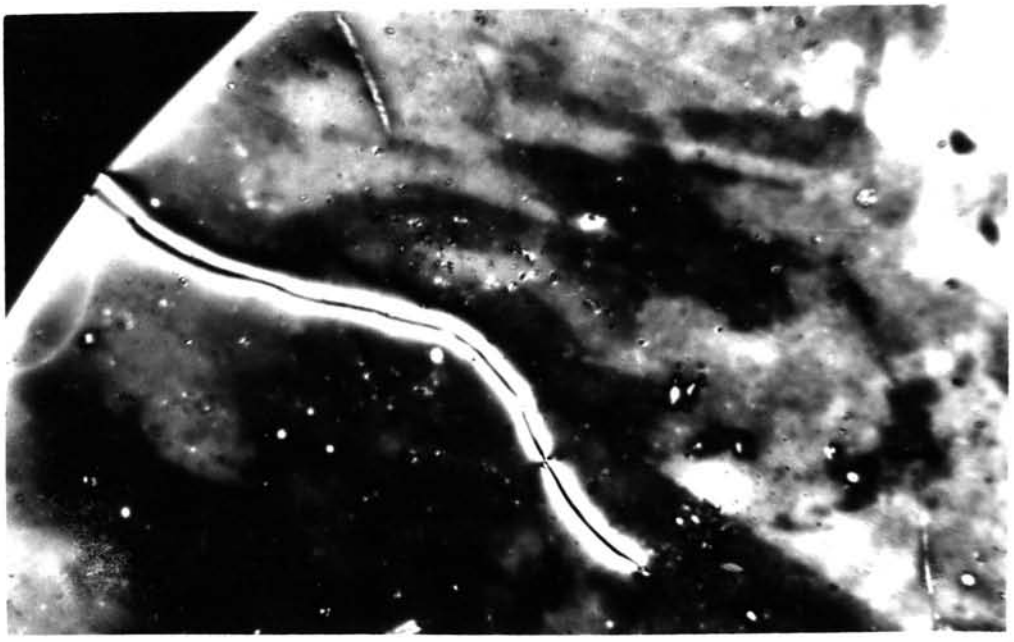

Fig.9a Inversion walls of the first kind formed by PDBAB at 135.3°C. Crossed polarizers.

Fig.9b Inversion walls of the second kind joining the $+\frac{1}{2}$ and $-\frac{1}{2}$ point singularities of MBBA(dirty) at 41.35°C. Crossed polarizers.

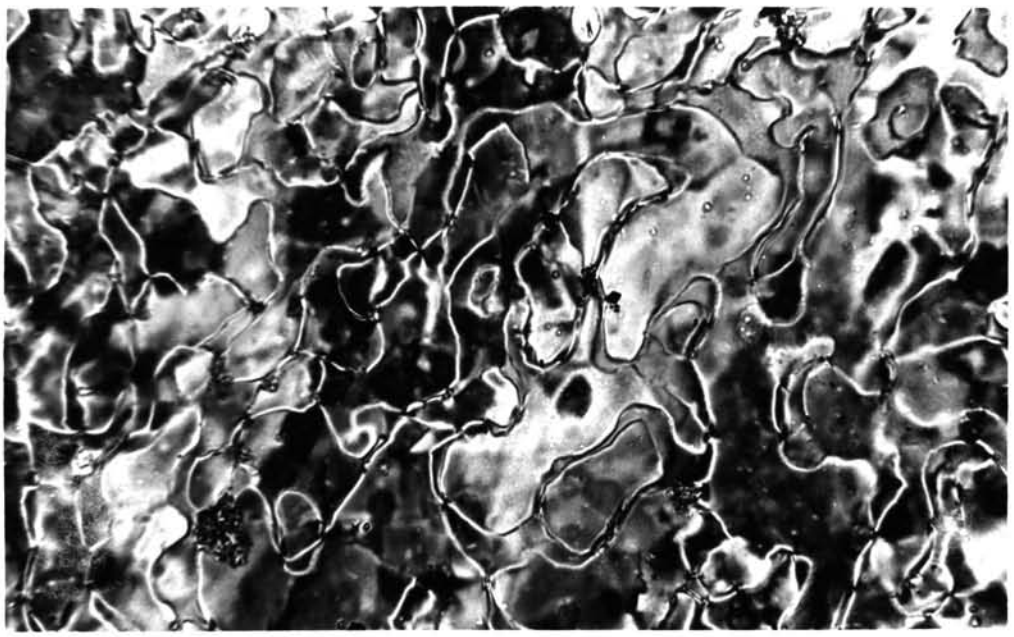

Fig.10 Schlieren texture of PDBAB at 134.9°C on a dirty slide. Inversion lines are formed by displacing the cover slip.

iii. Observation on nematic-nematic mixtures.

The microscopic textures of thin films of the following nematic-nematic mixtures were studied:

EPP-Hep/PAA, EPP-Hep/EPP-Hex and EPP-Hep/BEPCPC.

Every composition of EPP-Hep and EPP-Hex exhibited the same texture as in the pure components. No schlieren texture was observed near the transition temperature (see Fig.11). For the system EPP-Hep/PAA and EPP-Hep/BEPCPC, the marbled textures exhibited by the mixtures were not so different from those of the pure components. But near the nematic-isotropic transition temperature, the schlieren texture was observed

near the isotropic surface and lines of discontinuity appeared. It is noticeable that the schlieren brushes and the line discontinuities in the mixtures were not so smooth as in the pure substances; they were in fact very distorted (Figs.12a and 12b). The brushes around the singular points were short and narrow. The mixtures had a high tendency to show the pseudo-isotropic texture.

Figs.13a and 13b show the texture of PAA/EPP-Hep 50% at 114.3°C and 114.6°C on cooling from the isotropic to the nematic phase. The partially pseudo-isotropic state was always observed near the transition temperature. On cooling from the isotropic to the nematic phase, dark drops (under crossed polarizer) with white edges were formed. When the drops touched each other, the bright touching lines from the joining edges of the drops were rapidly eliminated. After the partially pseudo-isotropic state was formed, spherulites were slowly created within the mesomorphic layer. Some spherulites were large and some were small. As the temperature was decreased, the nearby spherulites,which always contained point singularities of the same sign, touched each other. Their dark brushes joined together and a new point singularity of the opposite sign was created at the touching point with two other brushes along the touching edges. As the polarizer was rotated, the brushes of the new singularity rotated in the opposite direction with respect to the original

ones. Merging of the new singularity with either of the original ones took place and a larger spherulite with only one point singularity was left. These spherulites always contained point singularities of the same sign.

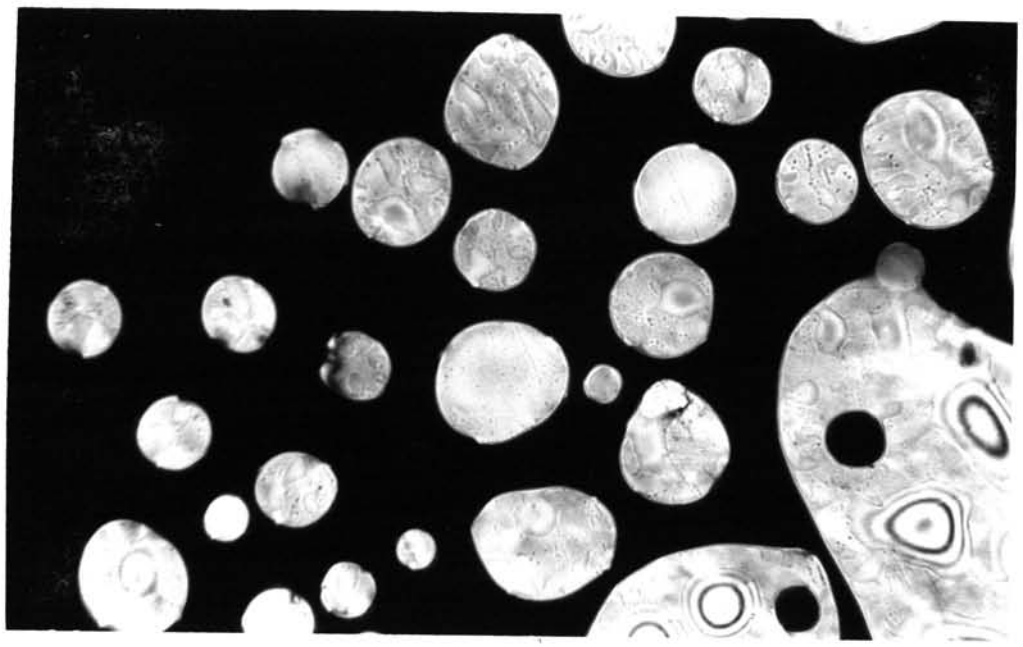

Fig.11 Texture of EPP-Hex/EPP-Hep 80% at 120.25°C
Crossed polarizers.

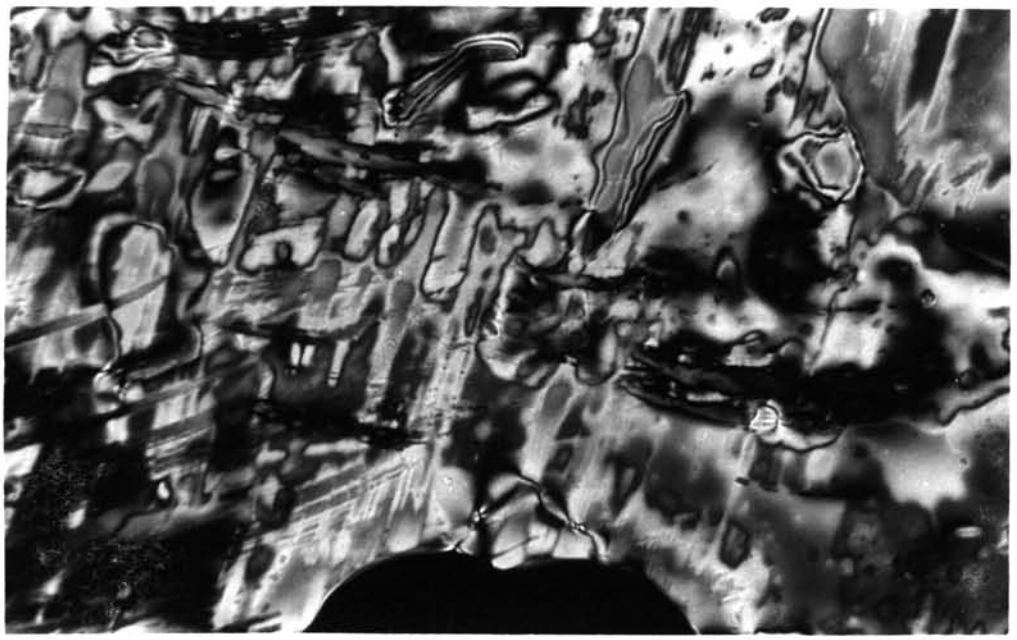

Fig.12a Texture of EPP-Hep/PAA 20%, at 113.55°C.

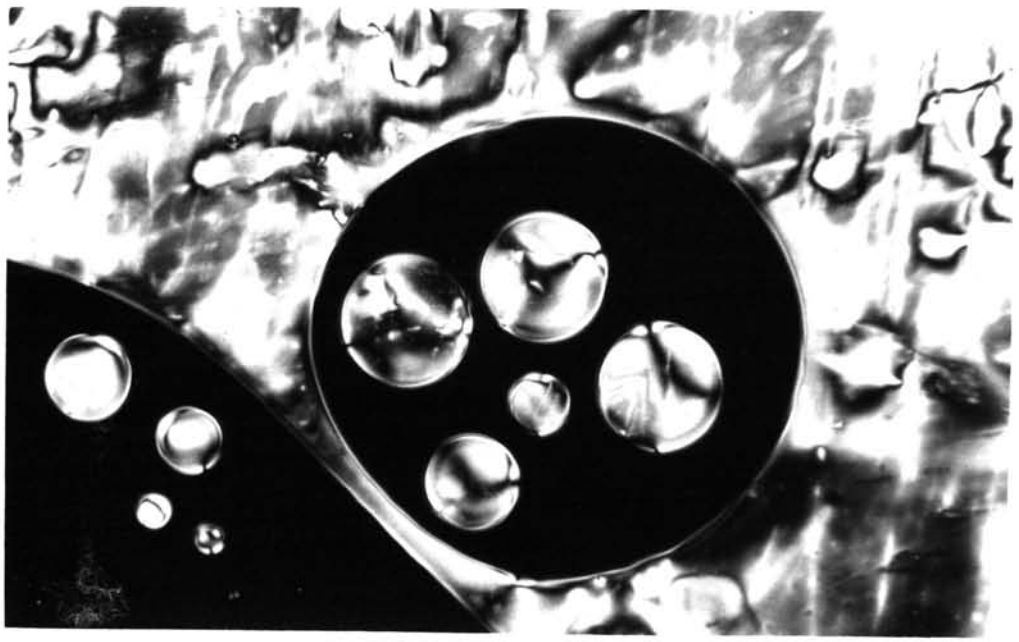

Fig.12b Texture of EPP-Hep/PAA 20% at 113.7°C.

Fig.13a Partially pseudo-isotropic texture of PAA/EPP-Hep 50% at 114.3°C. Crossed polarizers.

Fig.13b Spherulites formed in the partially pseudo-isotropic state of PAA/EPP-Hep50% at 114.6°C. Crossed polarizers.

iv. Observation of nematic droplets.

Nematic droplets were not always observed at the isotropic-nematic transition. In the cases of EPP-Hep and EPP-Hex (recryst.), when the specimen was cooled slowly from the isotropic, the nematic region slowly swept from the slide edge and no nematic droplets were formed. However, when the heating rate was high, droplets were formed. The droplets were not round, and had marbled texture inside them. The droplets appeared to stick to the glass surface and to grow rapidly at constant temperature.

In other nematogenic substances, droplets with dark brushes were usually observed. Some droplets appeared with distinct crosses which rotated as the polarizer around a point singularity in the middle of each droplet. Some droplets contained two point disclinations of opposite signs with the brushes pointing in the opposite directions. Some had only one point disclination but some had three. The edges of these droplets always showed higher birefringence than the other parts. The point singularities changed their positions as the size of the droplets increased.

At a constant temperature, the droplets which were properly nucleated started to grow rapidly at the beginning, the rate of growth then gradually decreased, and the droplets appeared to stop growing any further when a certain size was attained. As the temperature was decreased, the drops grew

further and touched each other. It was not observed that there was a definite tendency of the droplets touching at the point singularities. When the droplets touched, sharp bright lines or sometimes dark lines, appeared at the boundary and then disappeared in a moment. A point singularity of one brush in each drop always moved towards the nematic surface. It is surprising that this kind of singularity was only found at the nematic surface. If the droplets touched at the point singularities, the latter would either annihilate each other or create a new singularity depending on the types of the original singularities. A singularity with two brushes was created from the coalescence of two one-brush singularities of the same sign. The singularities with four brushes characteristic of the schlieren texture resulted from the emerging of half integral singularities of the same sign. In addition, this type of singularity was sometimes obtained when the ends of the brushes of whole-numbered singularities of the same sign touched. Two brushes were created at the boundary and intersected the original ones at the created point singularity. Generally, sharp bright lines were formed at the boundary instead of the point singularities of opposite signs.

From Fig.14 showing the nematic droplets of PDBAB at 136.3°C, it should be noticed that the brushes possessed by the point singularities of the same sign almost point in parallel directions.

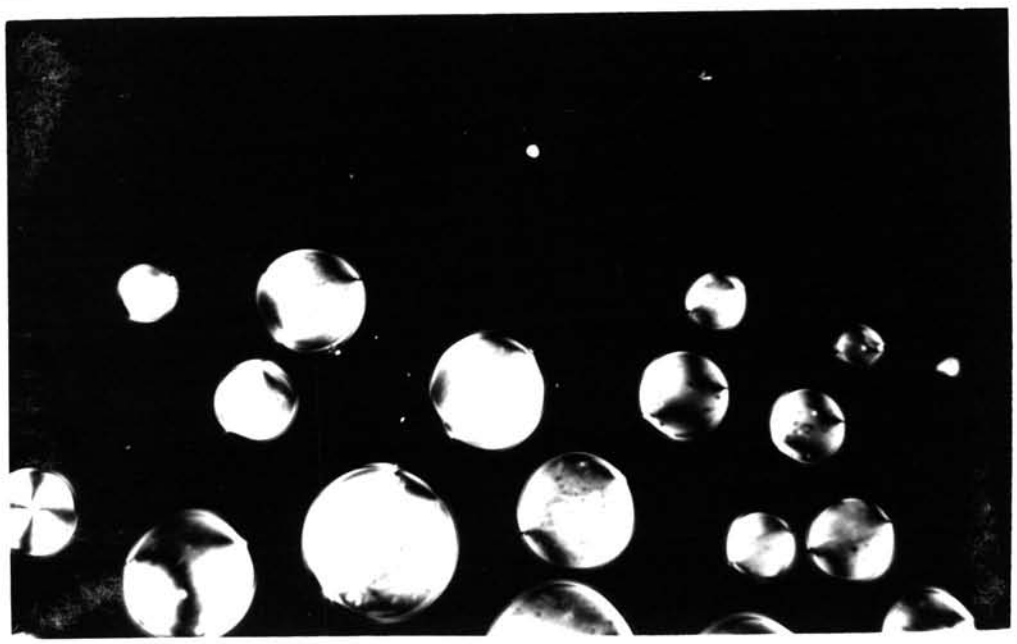

Fig.14 Nematic droplets of PDBAB at 136.3°C. Crossed polarizers.

II.5.3 Investigation of the growth of nematic droplets.

The rates of growth of the nematic droplets of various compounds and of nematic-nematic mixtures were determined. The maximum size of droplets depended on the melting temperature of the substance and the temperature difference from the isotropic point. The larger the temperature difference was, the larger was the number of droplets grown and the smaller were the sizes of the droplets. In recrystallized samples the shapes of the droplets were not so round and their growth rates were not uniform. These droplets were very sensitive to temperature gradient; indeed even local fluctuations in temperature of the order of .01°C would affect the size of the droplets considerably.

Experimentally, the size of the droplets and the time could be related by the empirical relation:

$$D \propto t^n$$

where D = diameter of droplets in an arbitrary unit

t = time(sec)

n = positive number < 1

The experimental results are shown in the following tables and graphs.

i. Tables of growth rates of nematic droplets.

Table 4 Growth rates of nematic droplets of PAP at 165.9°C (These droplets were not round.)

t (sec) \ no. of exp.	DIAMETER (x 80 μm)				
	1	2	3	4	5
0	.60	.40	.50	.50	.70
10	.80	1.30	.90	.90	.90
20	.90	2.30	1.15	1.20	1.10
30	1.25	2.50	1.30	1.40	1.45
45	1.80	3.00	1.40	1.50	1.80
60	2.15	3.40	1.45	1.80	2.10
75	2.30	3.90	1.50	2.10	2.30
90	2.60	4.10	1.55	2.20	2.50
105	2.90	4.10	1.60	2.20	2.90

Table 5 Growth rates of nematic droplets of PDBAB at 135.8°C

t (sec) \ no.of exp.	DIAMETER (x 80 μm)				
	1	2	3	4	5
0	.10	.10	.30	.60	.30
10	.45	.30	.45	.80	.50
20	.60	.45	.60	1.0	.70
30	.80	.55	.70	1.10	.80
45	1.00	.70	.80	1.30	.90
60	1.20	.85	.90	1.50	1.00
75	1.40	.95	1.00	1.65	1.10
90	1.55	1.10	1.15	1.85	1.20
120	1.80	1.20	1.30	2.10	1.20
n	0.7±0.1	0.7±0.1	0.6±0.05	0.8±0.01	0.4±0.04

Table 6 Growth rates of nematic droplets of PAD at 161.9°C.

t (sec) \ no.of exp.	DIAMETER (x 80 μm)				
	1	2	3	4	5
0	.20	.20	.60	.90	.40
10	.40	.90	.70	1.10	.65
20	.50	1.35	.75	1.40	.90
30	.60	1.65	.80	1.55	1.10
45	.75	2.20	.85	1.80	1.35
60	.80	2.65	.90	1.95	1.45
75	.90	2.90	.95	2.00	1.55
105	1.05	3.40	1.00	2.00	1.70
n	0.5±0.1	0.5±0.1	0.3±0.1	0.3±0.05	0.3±0.05

Table 7 Growth rates of nematic droplets of PAA at 134.2°C.

t (sec) \ no. of exp.	DIAMETER (x 80 μm)				
	1	2	3	4	5
0	.20	.30	50	.40	.40
10	.40	.40	.90	.55	.70
20	.50	.45	1.10	.75	.95
30	.60	.50	1.25	.85	1.00
45	.70	.55	1.35	1.00	1.05
60	.75	.58	1.45	1.30	1.10
75	.80	.60	1.45	1.30	1.10
n	0.3±0.05	0.3±0.05	0.2±0.10	0.5±0.05	0.2±0.05

Table 8 Growth rates of nematic droplets of EPP-Hep/PAA 30% at 112.6°C.

t (sec) \ no. of exp.	DIAMETER (x 80 μm)				
	1	2	3	4	5
0	.70	.30	. 20	.30	.45
10	.95	.60	. 60	.80	.80
20	1.10	.80	.70	1.10	.95
30	1.20	.90	.85	1.20	1.10
45	1.40	1.05	.95	1.25	1.30
60	1.50	1.20	1.00	1.30	1.50
75	1.80	1.30	1.00	1.35	1.55
90	2.00	1.40		1.40	1.58
105	2.10	1.45		1.40	1.60
120	2.30	1.50			
n	0.6±0.05	0.3±0.05	0.3±0.05	0.2±0.05	0.5±0.07

Table 9 Growth rates of nematic droplets of EPP-Hep/PAA50% at 114.9°C

t (sec) \ no. of exp.	DIAMETER (x80 μm)				
	1	2	3	4	5
0	.50	.20	.50	.50	.40
10	.90	.50	.75	.90	.60
20	1.10	.70	.90	1.00	.75
30	1.20	.75	1.00	1.10	.85
45	1.20	.82	1.00	1.10	.85
60	1.20	1.10	1.00		
75	1.20	1.20	1.00		
n	0.25±0.05	0.5±0.1	0.3±0.05	0.2±0.05	0.5±0.05

Table 10 Growth rates of nematic droplets of EPP-Hep/PAA 80% at 122.7°C.

t (sec) \ no. of exp.	DIAMETER (x 80 μm)				
	1	2	3	4	5
0	.50	.40	.30	.35	.30
10	.70	.65	.60	.45	.50
20	.80	.70	.70	.50	.60
30	.82	.75	.75	.52	.65
45	.85	.78	.80	.52	.70
60	.85	.78	.85		.75
n	0.1±0.05	0.1±0.05	0.2±0.05	0.2±0.05	0.25±0.1

ii. Graphs of diameter of droplets versus time

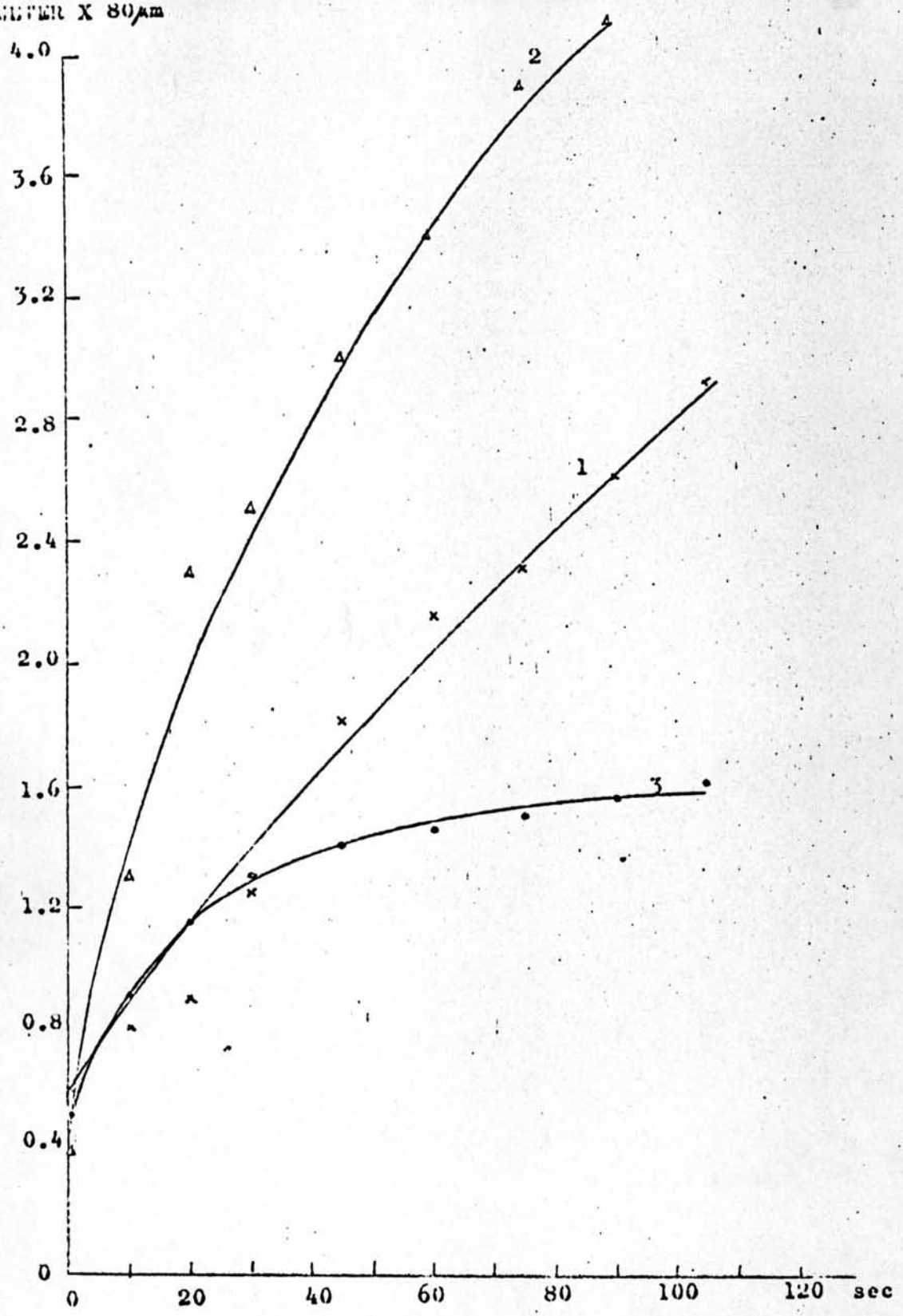

Fig.15a Time-Diameter Curves of PAP

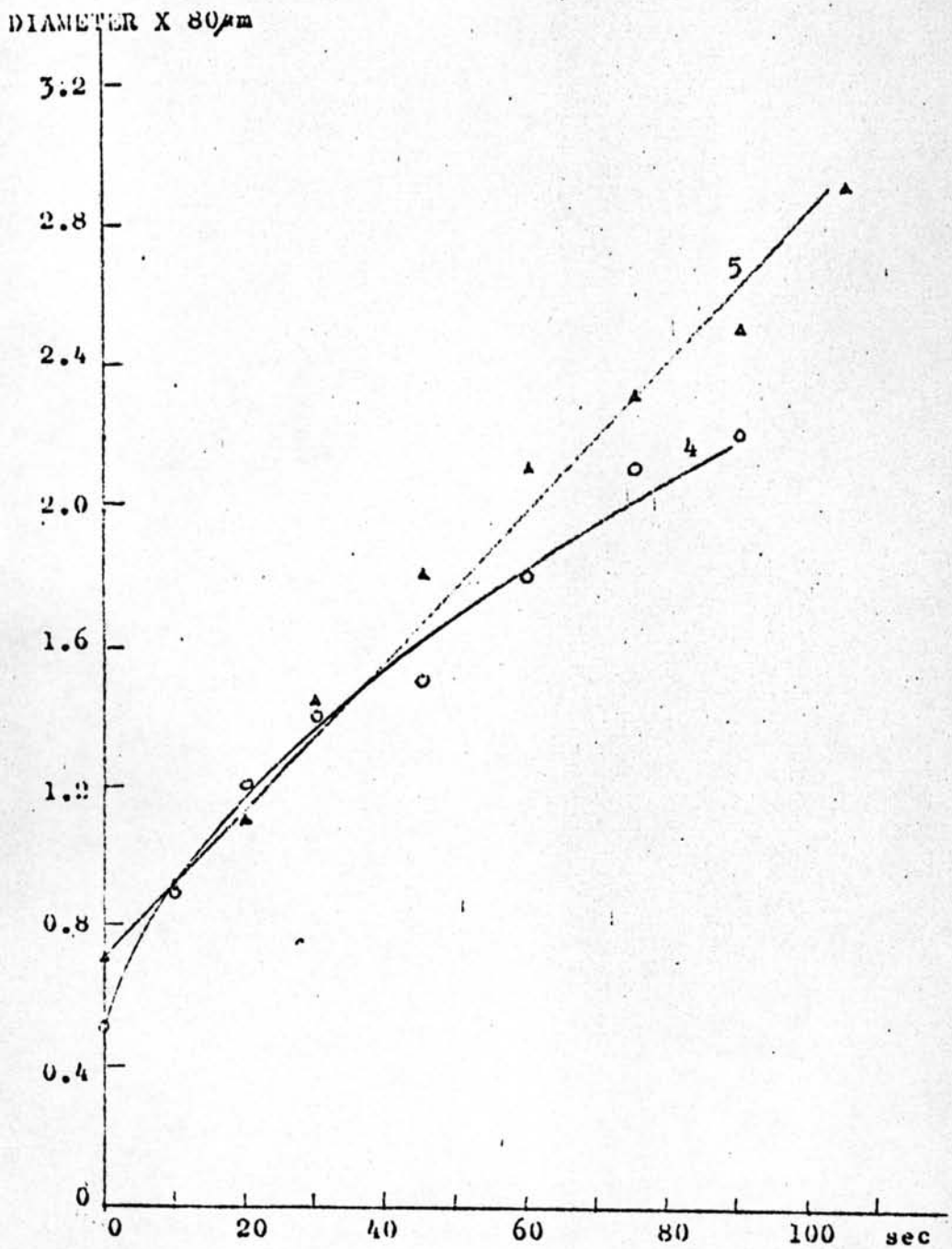

Fig.15b Time-Diameter Curves of PAP

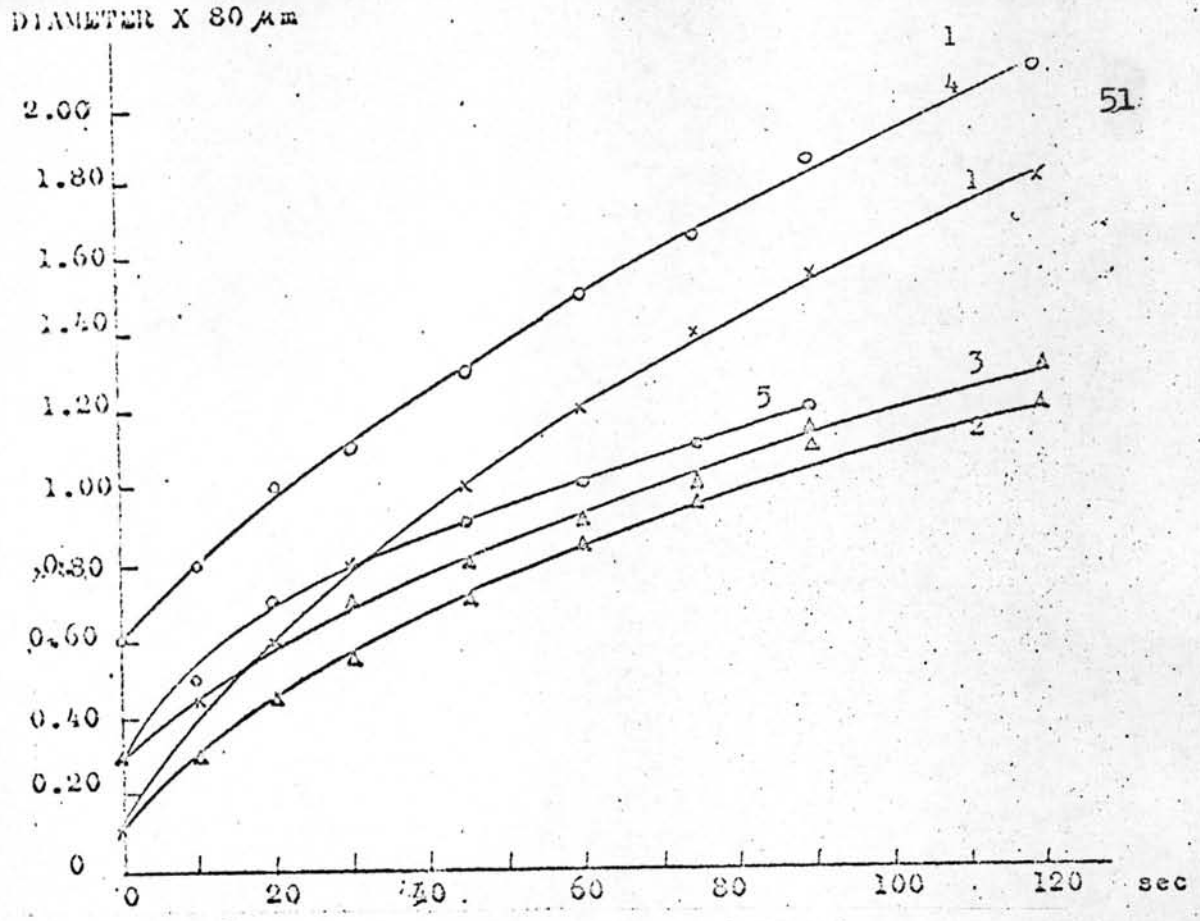

Fig.16a · Time-Diameter Curves of PDBAB

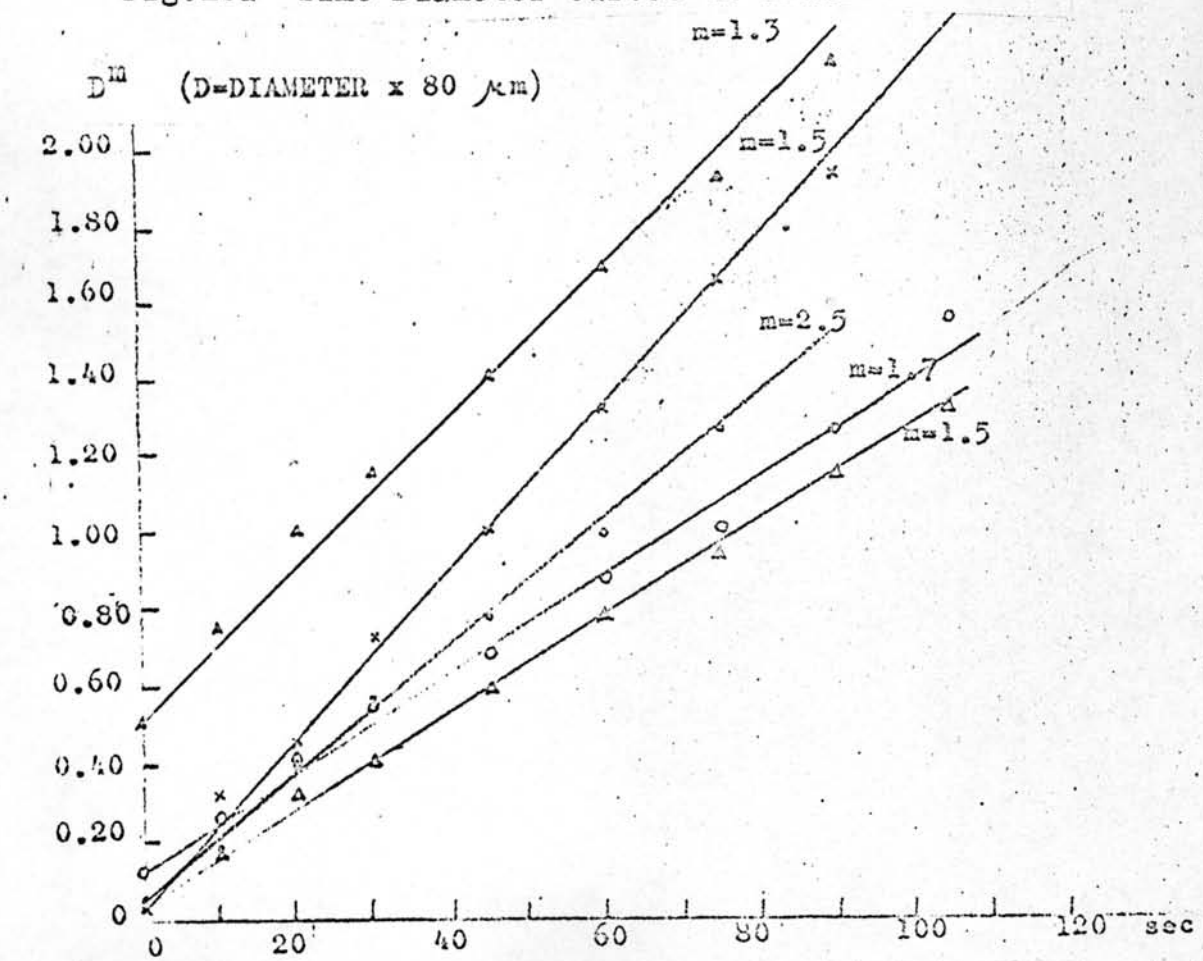

Fig.16b Time-(Diameter)^m curves of PDBAB

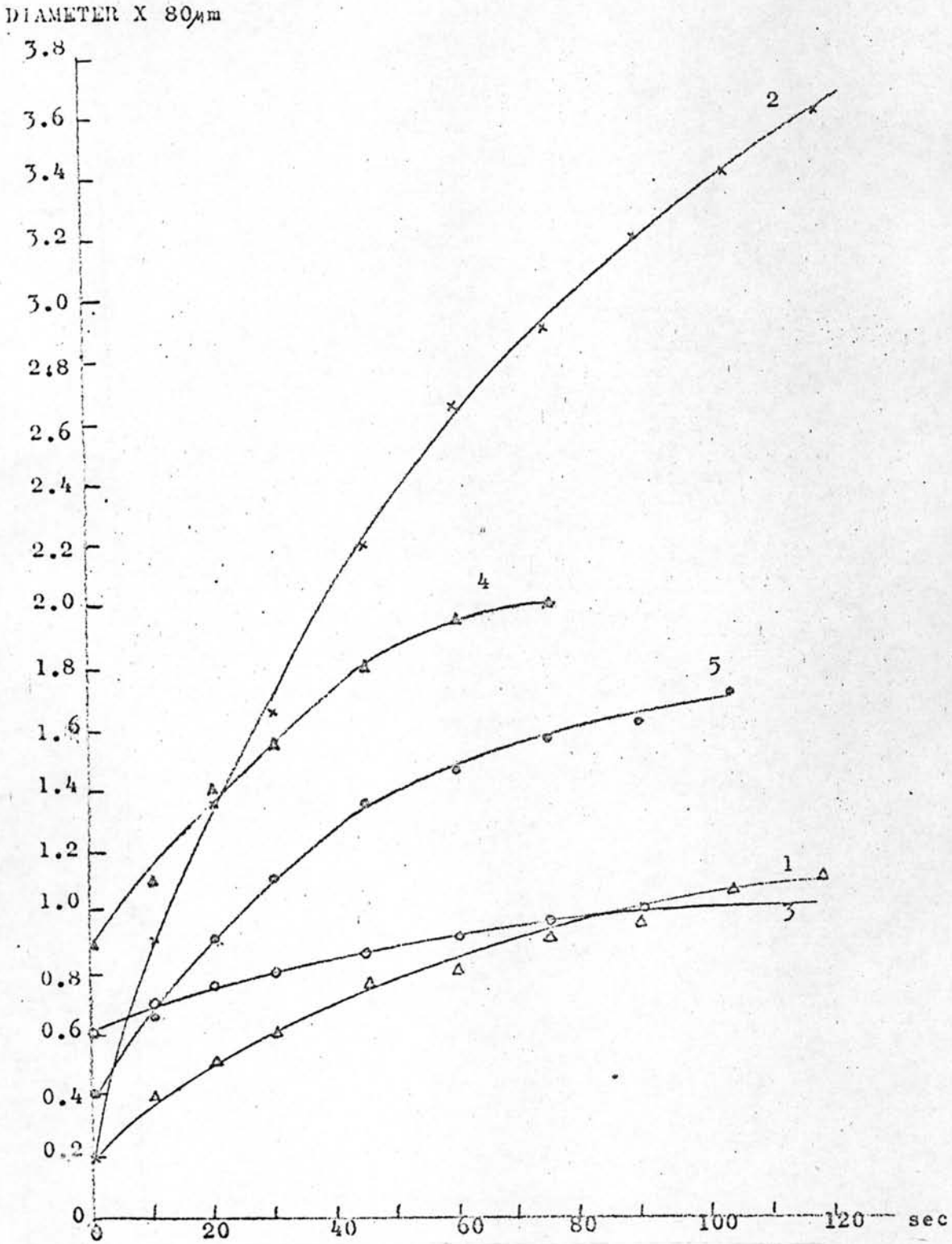

Fig.17a Time-Diameter curves of PAD

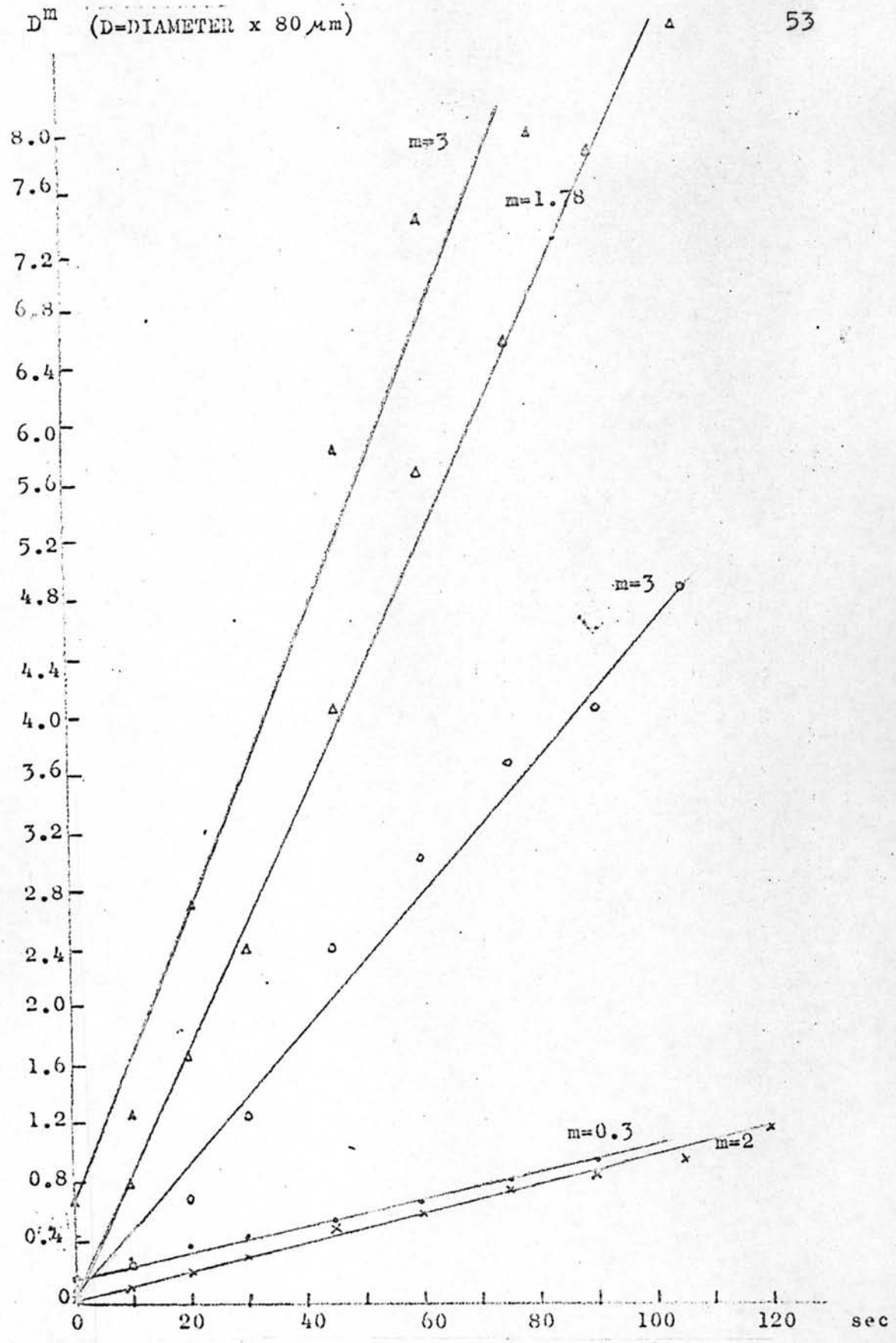

Fig.17b Time-(Diameter)^m curves of PAD

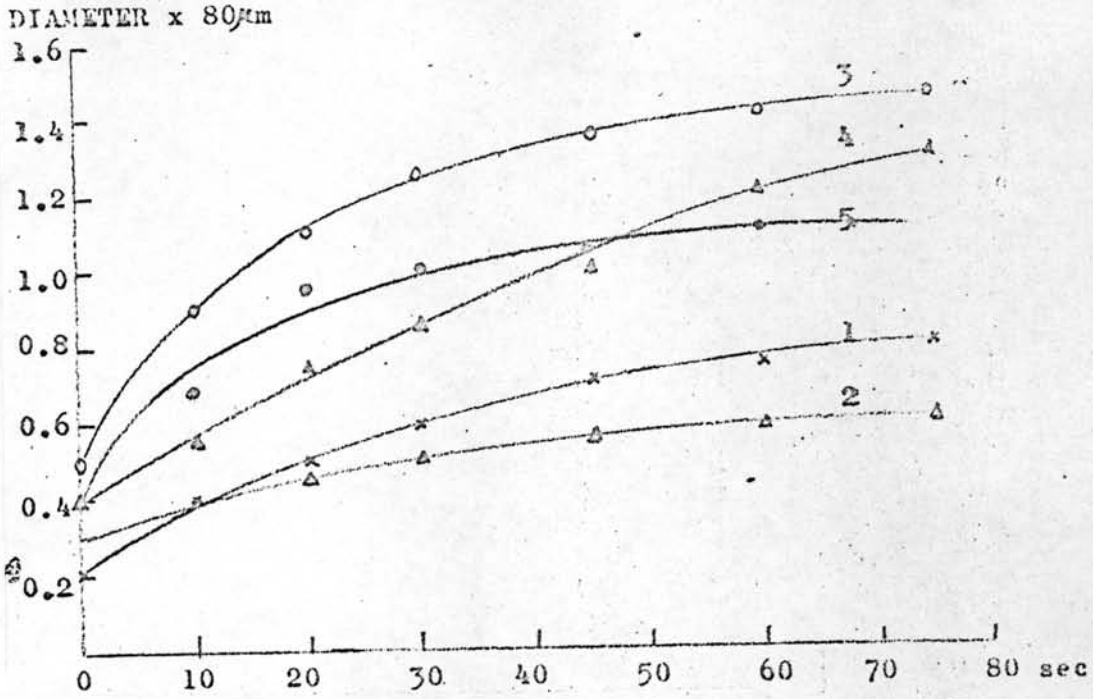

Fig.18a Time-Diameter Curves of PAA

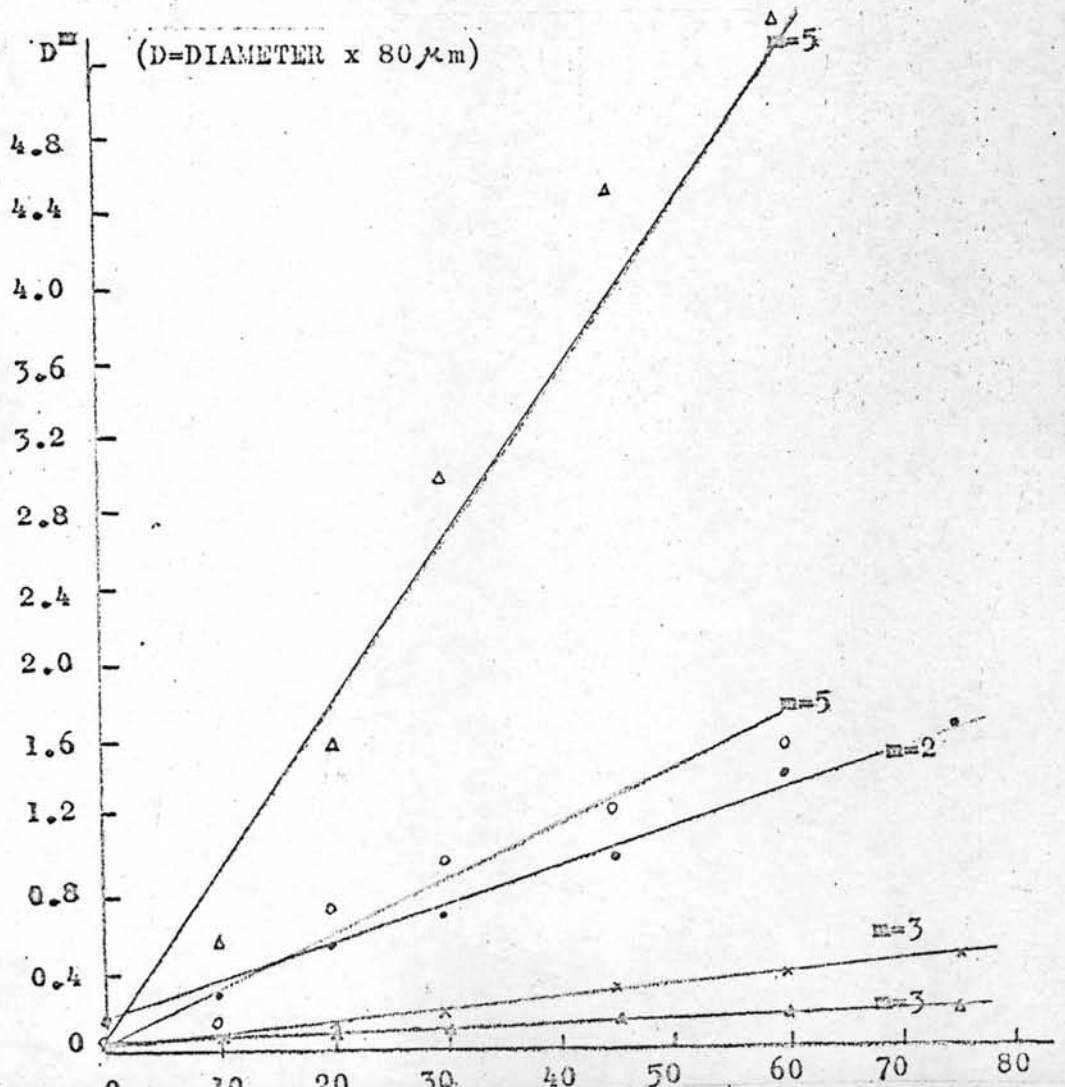

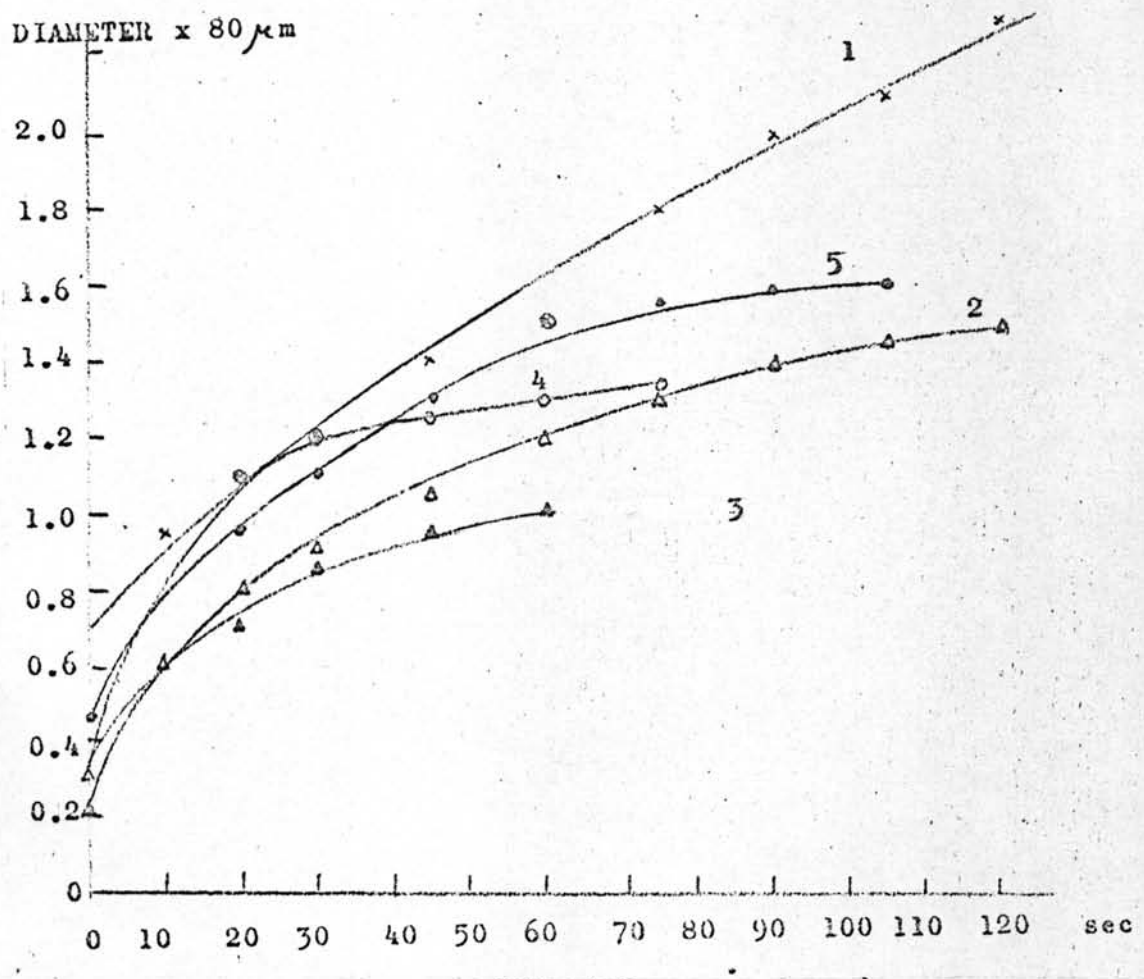

Fig.19a - Time-Diameter Curves of EPP-Hep/PAA 30%

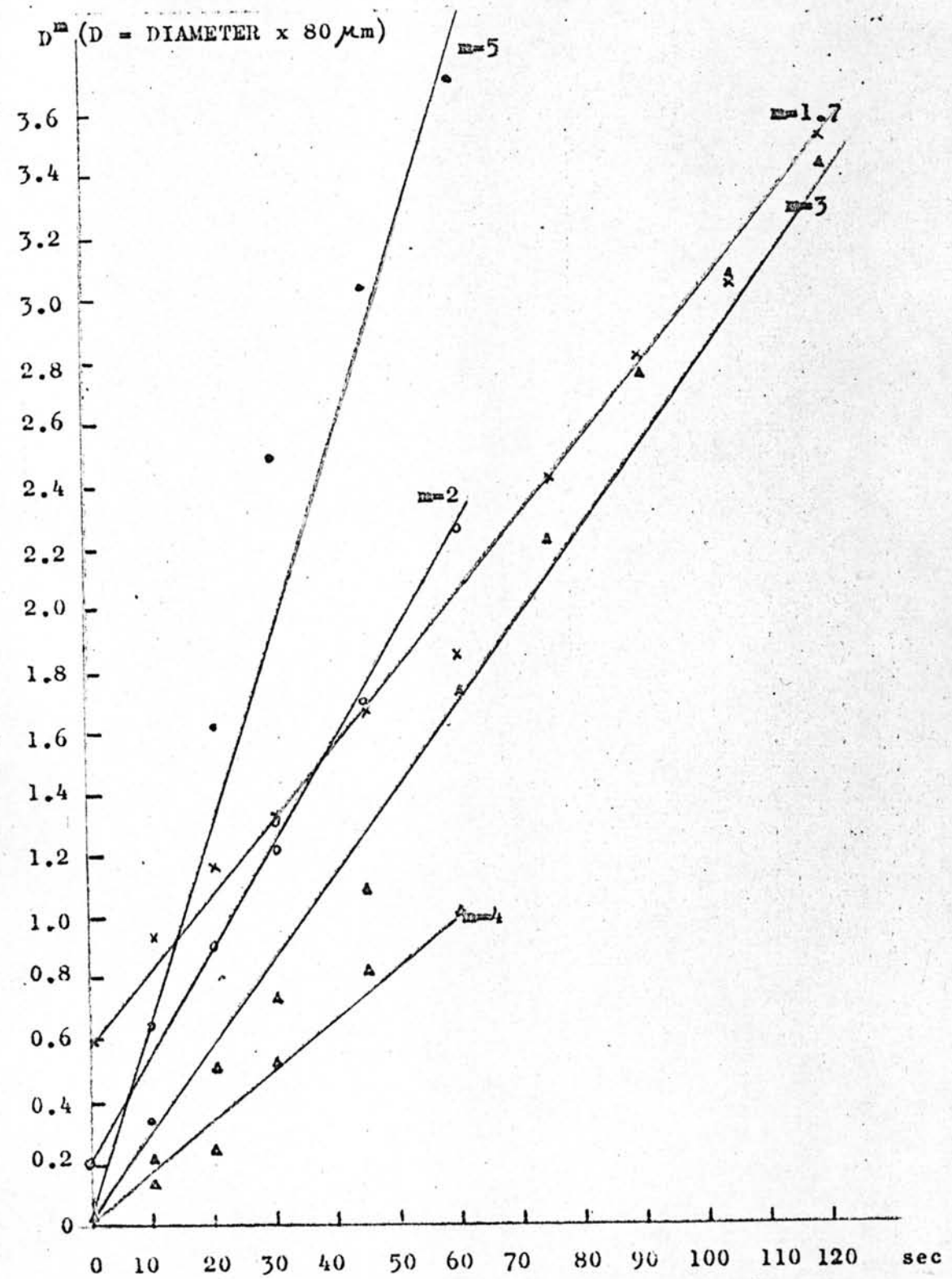

Fig.19b Time-(Diameter)^m Curves of EPP-Hep/PAA 30%

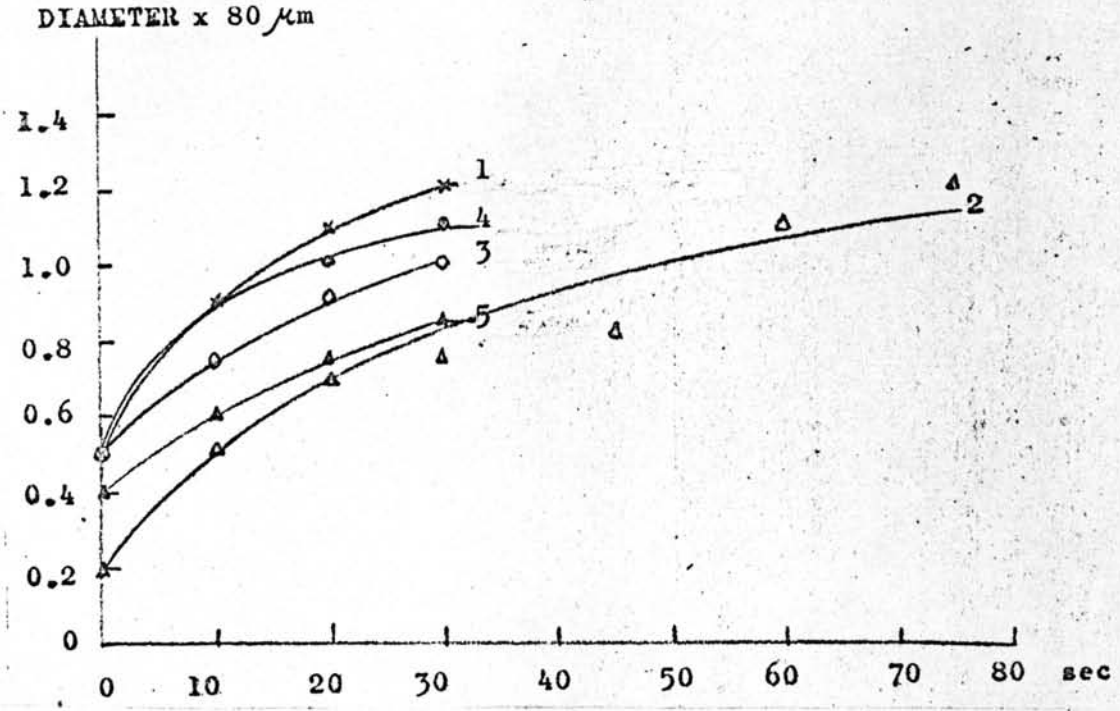

Fig.20a Time-Diameter Curves of EPP-Hep/PAA 50%

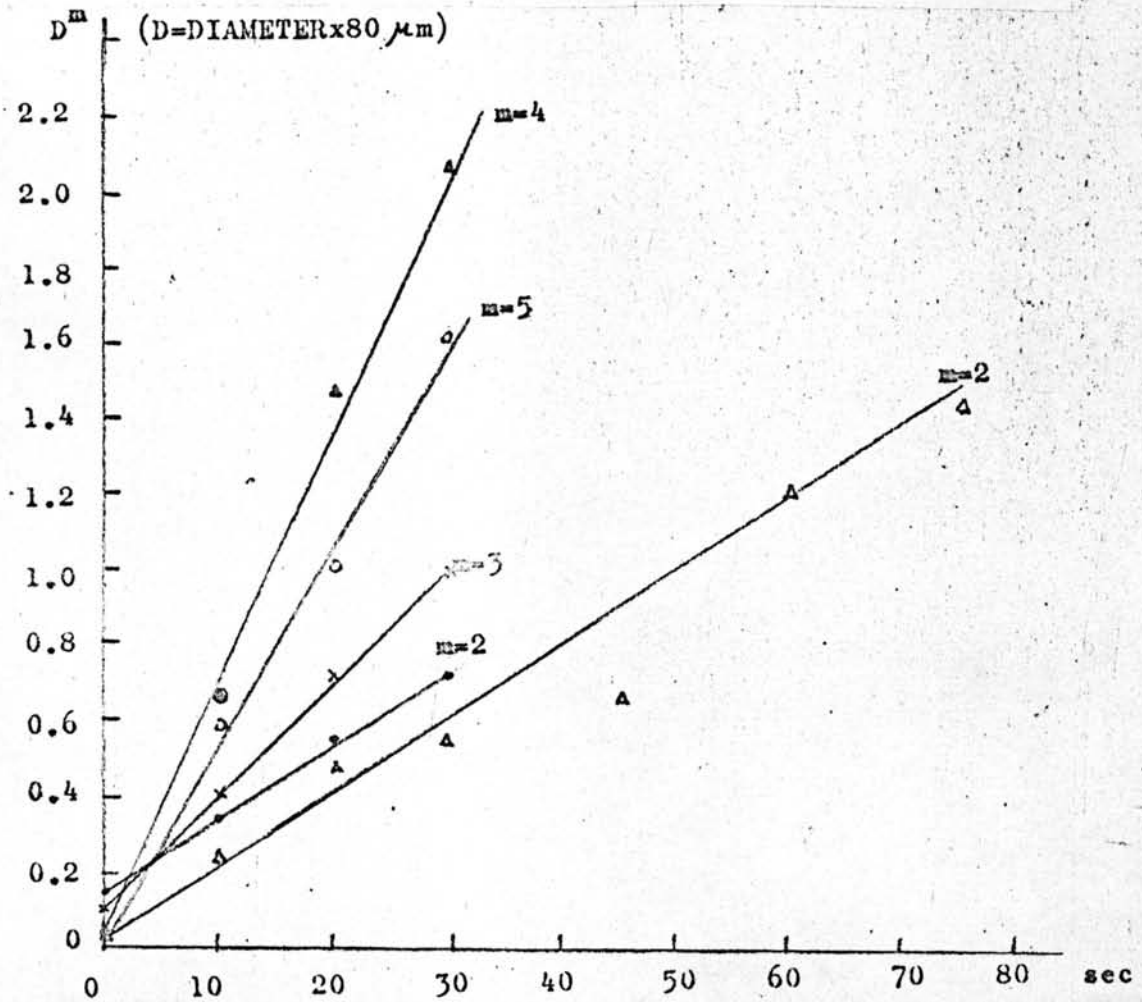

Fig.20b Time-(Diameter)^m Curves of EPP-Hep/PAA 50%

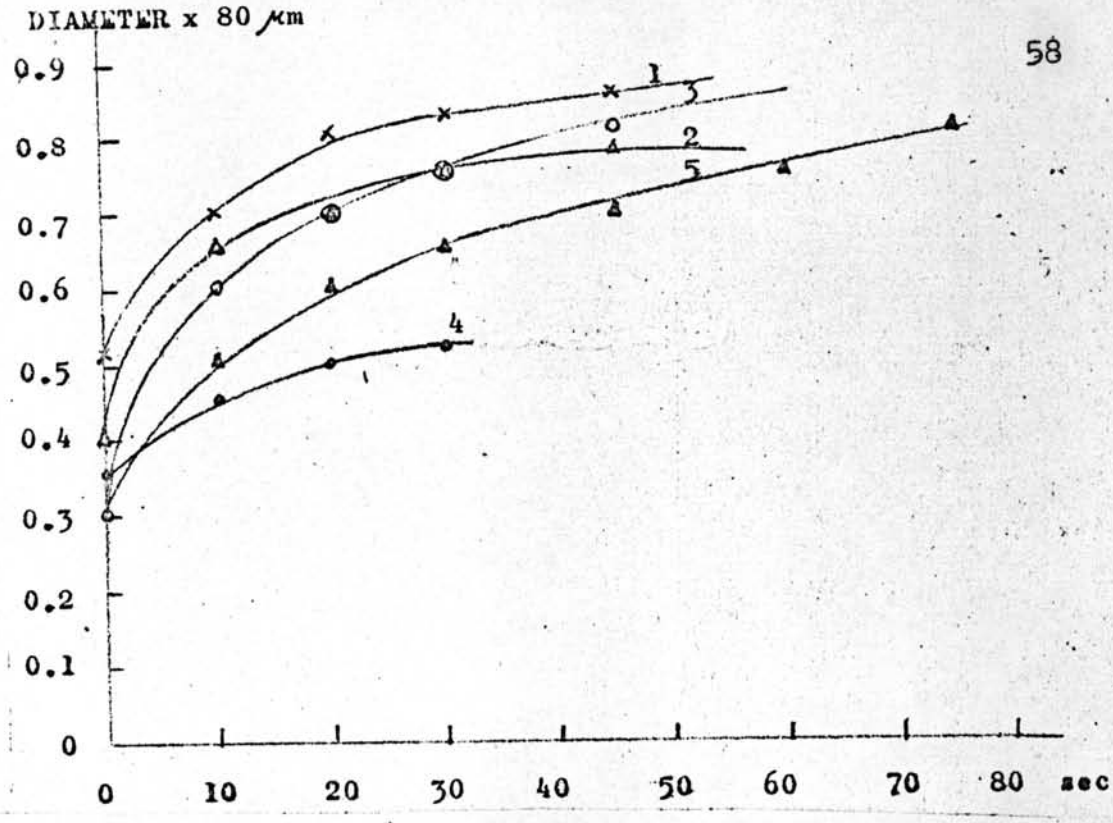

Fig.21a Time-Diameter Curves of EPP-Hep/PAA 80%

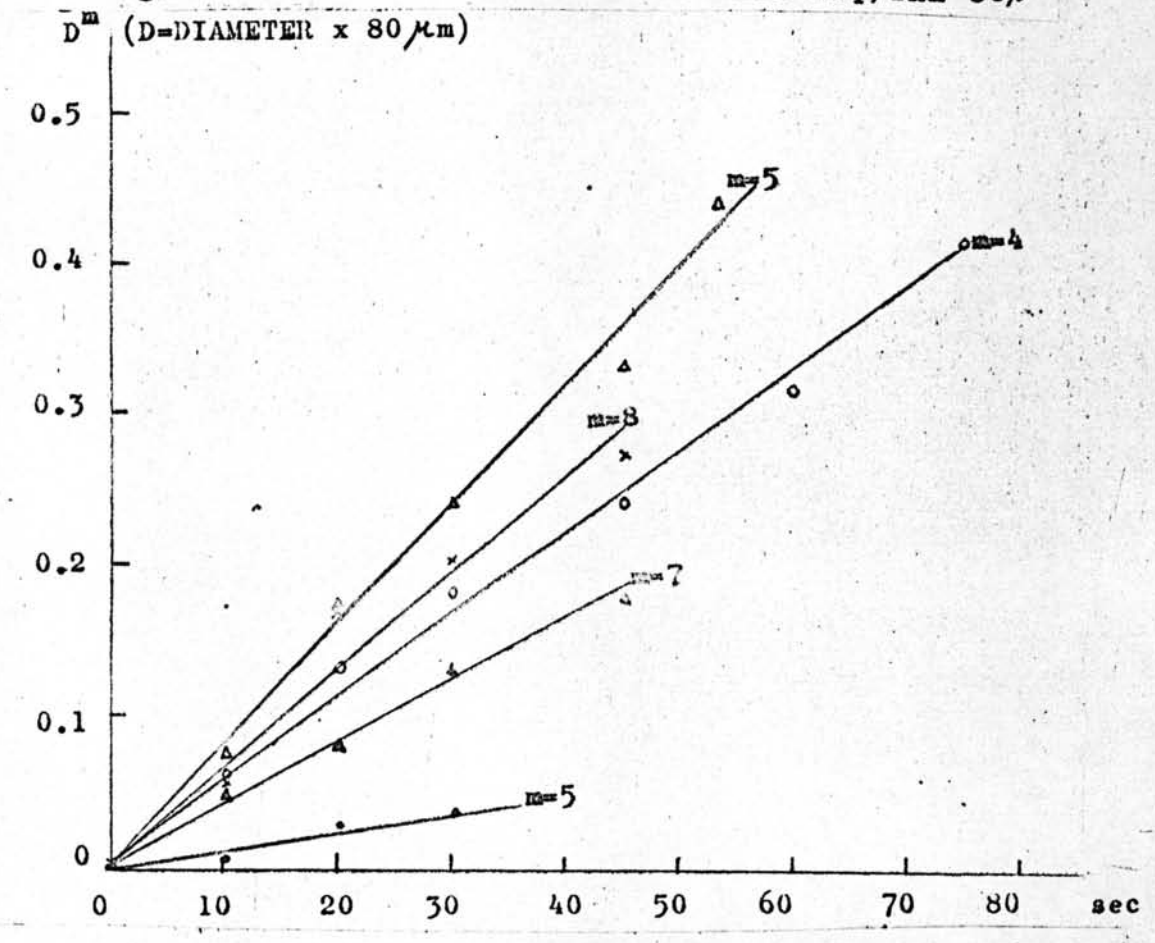

Fig.21b Time-(Diameter)^m Curves of EPP-Hep/PAA 80%

II.5.4 Limits of inaccuracy.

The limit of possible inaccuracies in the temperature control on the Mettler FP52 heating stage was within 0.02°C. throughout the present experiments.

The inaccuracy in the determination of the size of nematic droplets could have arisen from the following:

1. The scale of the microscope vernier on the eyepiece was rough, the precise reading was 80 μm, the next figure being insignificant. The possible errors from the scale reading were about 20-30 μm.

2. A bright line was always observed around the edge of a droplet and it could not be focussed into a sharp line. Thus possible errors always occurred within the limit of about a few microns, equal to the width of this line.

3. Thermal fluctuation played an important part on the growth rate. Even small fluctuations of temperature would change the size of the droplets considerably and would cause a nonuniform growth rate.